INVESTIGATION OF AMINOETHYL METHACRYLATE POLYMERS FOR IN VIVO DELIVERY OF mRNA

A Thesis Submitted to
The Graduate School of Engineering and Sciences of İzmir Institute of Technology
in Partial Fulfillments of Requirements for Degree of

MASTER OF SCIENCE

in Bioengineering

by
Ayça ESMER

July 2024
İZMİR

We approve the thesis of **Ayça ESMER**

Examining Committee Members:

Prof. Dr. Volga BULMUŞ
Bioengineering, İzmir Institute of Technology

Prof. Dr. Hatice Güneş ÖZHAN
Molecular Biology and Genetics, İzmir Institute of Technology

Assoc. Prof. Dr. Ahmet AYKAÇ
Bioengineering, İzmir Katip Çelebi University

09 July 2024

Prof. Dr. Volga BULMUŞ
Supervisor, Bioengineering, İzmir Institute of Technology

Assoc. Prof. Ceyda ÖKSEL
Head of the Department of Bioengineering

Prof. Dr. Mehtap EANES
Dean of the Graduate School of Engineering and Sciences

ACKNOWLEDGMENTS

I would like to express my deepest appreciation to my supervisor Prof. Dr. Volga Bulmuş for her support and instructiveness. Working in her laboratory was an excellent experience for me. I am grateful to all my colleagues in the laboratory for their support and help. I am grateful to the Scientific and Technological Research Council of Türkiye (TÜBİTAK) for their financial support, which I received support from within the scope of the 2210-C Domestic Graduate Scholarship Program, and Izmir Institute of Technology for BAP-AÜDP grant 2022 İYTE-2-0038. I would also like to extend my deepest gratitude to Prof. Dr. Hatice Güneş Özhan for seeing me as her student and supporting me. It would not have been possible without the support of Esra Katkat, whom I worked with at IBG. I would like to thank everyone I met at IBG for the opportunities they provided me and for their friendliness. I also would like to thank my committee members Prof. Dr. Hatice Güneş Özhan and Assoc. Prof. Dr. Ahmet Aykaç.

Words cannot express my gratitude to my family for their limitless love, motivation, and moral support. Finally, my biggest thanks to myself for being able to fight against all the difficulties, never giving up, and believing in hard work. I am grateful for everything.

ABSTRACT

INVESTIGATION OF AMINOETHYL METHACRYLATE POLYMERS FOR *IN VIVO* DELIVERY OF mRNA

There is a tremendous need for non-viral vectors for safe and efficient gene therapies. Especially the use of polymeric vectors for messenger RNA (mRNA) based gene therapies is limited. Within the scope of this thesis, it is aimed to perform a preliminary investigation on the *in vivo* transfection ability of a newly developed polymeric vector using zebrafish embryos in comparison with well-known lipidic and polymeric vectors. In line with this goal, the mRNA transfection ability of the block copolymer, poly(oligo(ethylene glycol) methacrylate)-*b*-poly(2-(amino)ethyl)amino)ethyl methacrylate, $P(OEGMA)_{42}$-b-$P(AEAEMA)_{48}$ along with Lipofectamine 3000 and branched polyethylene imine (PEI) (25 kDa) was examined *in vivo* on zebrafish embryos. A number of optimization experiments were first performed using naked mRNA or Lipofectamine-mRNA complexes to determine the best administration site and method, mRNA dose, type and development stage of embryos within the studied range. Considering the results obtained from optimization experiments, polyplexes formed with GFP-mRNA (2000 ng) and $P(OEGMA)_{42}$-b-$P(AEAEMA)_{48}$ at an N/P ratio of 3.6 or 7.3 were injected into the pericardial cavity of developing zebrafish embryos at 48 hours post fertilization to observe GFP expression. Naked mRNA, naked embryos, Lipofectamine-mRNA complex, and PEI-mRNA polyplexes were used for comparison. Samples were visualized 24 hours after injection using confocal microscopy and analyzed with Image J. The block copolymer showed transfection efficiency comparable with the golden standard polymeric vector PEI. The preliminary results obtained in this study pave the way for further investigations on the *in vivo* applications of $P(OEGMA)_{42}$-b-$P(AEAEMA)_{48}$ as a potential polymeric vector for mRNA-based gene therapies.

ÖZET

mRNA TAŞIMASI İÇİN AMİNOETİL METAKRİLAT POLİMERİN *İN VİVO* ARAŞTIRILMASI

Güvenli ve etkili gen tedavileri için viral olmayan vektörlere büyük bir ihtiyaç vardır. Özellikle mRNA (mesajcı RNA) temelli gen tedavileri için polimerik vektörlerin kullanımı çok sınırlıdır. Bu tez kapsamında, zebra balığı embriyoları kullanılarak yeni geliştirilen bir polimerik vektörün *in vivo* transfeksiyon etkinliğinin, bilinen lipidik ve polimerik vektörlerle karşılaştırmalı olarak ön araştırmasının yapılması amaçlanmıştır. Bu amaç doğrultusunda, blok kopolimer, poli(oligo(etilen glikol) metakrilat)-b-poli(2-(amino)etil)amino)etil metakrilat, $P(OEGMA)_{42}$-b-$P(AEAEMA)_{48}$ ile Lipofectamine 3000 ve dallanmış polietilen iminin (PEI) (25 kDa) mRNA transfeksiyon etkinliği zebra balığı embriyoları modeli üzerinde *in vivo* olarak incelenmiştir. Çalışılan aralıkta en iyi uygulama bölgesi ve yöntemi, mRNA dozu, türü ve gelişim aşamasını belirlemek için önce çıplak mRNA veya Lipofectamine-mRNA kompleksleri kullanılarak birçok optimizasyon deneyi gerçekleştirildi. Optimizasyon deneylerinden elde edilen sonuçlar göz önünde bulundurularak, GFP-mRNA (2000 ng) ve N/P oranı 3.6 veya 7.3 olan $P(OEGMA)_{42}$-b-$P(AEAEMA)_{48}$ ile oluşturulan polipleksler, GFP ifadesini gözlemlemek için döllenmeden 48 saat sonraki gelişim aşamasında olan zebra balığı embriyolarının perikardiyal boşluğuna enjekte edildi. Karşılaştırma için çıplak mRNA, çıplak embriyolar, Lipofektamine-mRNA kompleksi ve PEI-mRNA polipleksleri kullanıldı. Örnekler enjeksiyondan 24 saat sonra konfokal mikroskobu kullanılarak görselleştirildi ve Image J ile analiz edildi. Blok kopolimer, altın standart polimerik vektör PEI ile karşılaştırılabilir transfeksiyon etkinliği gösterdi. Bu çalışmada elde edilen ön sonuçlar, mRNA tabanlı gen tedavileri için potansiyel bir polimerik vektör olarak $P(OEGMA)_{42}$-b-$P(AEAEMA)_{48}$'in *in vivo* uygulamaları üzerine daha fazla araştırma yapılmasının önünü açmaktadır.

TABLE OF CONTENTS

LIST OF FIGURES

Figure **Page**

Figure **Page**

Figure **Page**

Figure **Page**

LIST OF TABLES

Table **Page**

CHAPTER 1

INTRODUCTION

Gene-based therapies are being developed as a reliable and effective strategy for the treatment of many diseases including diabetes and cancer (Kamegawa et al. 2021, 7790). mRNAs have been widely investigated as an effective and reliable tool in gene-based therapies as they translate genetic information and enable the expression of proteins from genes (Zhang et al. 2021, 12181-12202). They are more reliable when compared to other types of nucleic acids because of several advantages. These include not requiring nuclear entry for genomic integration and transfection activity, enabling rapid protein expression even in nondividing or difficult to transfect cells, and providing predictable and consistent protein expression kinetics (Kim et al. 2021, 84-87). However, the large size, rapid degradation of mRNAs by nucleases, low uptake by cells and immunostimulatory effects limit the effective use of mRNAs in the clinical applications. In order to overcome these problems and develop mRNAs as a therapeutic tool, developing reliable and efficient carrier agents that condense mRNAs and protect them against nuclease enzymes, increase cellular uptake and shielding unwanted immunostimulatory effects is crucial. Carrier agents used in different gene based therapies do not show the same effect in mRNA based therapies due to the structural and dimensional differences between different types of nucleic acids. mRNA carrier vectors should be suitable to form stable complexes with large and flexible mRNA molecules (Sago et al. 2018, 6; Paunovska et al. 2022, 268-272).

Lipid-based nanocarriers have been widely used in mRNA based gene therapies. However, they possess important disadvantages including low stability, high cost, difficulty in modification, and unwanted premature release during storage and use (Ghasemiyeh & Mohammadi-Samani 2018, 289; Zhang et al. 2021, 12181-12202). In this direction, revealing the mRNA transport potential of polymers, which are more advantageous carrier agents compared to lipids, is very important for the dissemination of mRNA based therapies that have come to the fore in recent years. Cationic polymers

are being investigated as alternative carriers for nucleic acid therapeutics including mRNAs. Cationic polymers increase the serum stability of nucleic acids including mRNAs by forming polyelectrolyte complexes, i.e. polyplexes, as a result of electrostatic interactions with genetic material, facilitate cellular uptake and increase access to the endosome (Olden et al. 2018, 140-142; Pack et al. 2005, 582-587).

Various animal models have been employed to evaluate parameters such as biodistribution, toxic effects, and efficiency in preclinical studies of newly developed vectors. Rodents like mice and rats are commonly used in research due to their anatomical and genomic similarities to humans. However, they come with disadvantages such as high maintenance and development costs, and small progeny numbers. Zebrafish (*Danio rerio*) have emerged as a next generation *in vivo* animal model to address these challenges. Zebrafish share approximately 70% of their genome structure with humans (Martinez-Lopez et al. 2021, 7). They offer several advantages over other animal models, including transparent embryos, high fertility with rapid production cycles, simple and cost effective maintenance, ease of handling due to their small size, a short life cycle allowing for quick development of main organs, and a fully sequenced genome with controlled gene expression. These benefits make zebrafish an ideal model for various research fields.

Within the scope of this thesis, it is aimed to perform a preliminary *in vivo* investigation on the mRNA transfection ability of a newly developed polymeric vector, poly(oligo(ethylene glycol) methacrylate)-*b*-poly(2-(amino)ethyl)amino)ethyl methacrylate, $P(OEGMA)_{42}$-b-$P(AEAEMA)_{48}$ block copolymer, in comparison with well-known lipidic and polymeric vectors, using zebrafish embryos. Firstly, parameters such as zebrafish type (Casper type and AB type), embryonic developmental stage (0 hpf, 24 hpf, 48 hpf), injection site (pericardial cavity, trunk, circulation), and mRNA administration method were investigated separately. The GFP mRNA transfection ability of the block copolymer was then examined using the optimized experimental conditions in comparison with Lipofectamine and branched PEI (25 kDa). In the content of the thesis, following the literature summary in Chapter 2, Chapter 3 presents the materials, instruments and methods used. The results of the experiments performed are presented in Chapter 4.

CHAPTER 2

LITERATURE REVIEW

2.1. Gene Therapy

Gene therapy is a potent therapeutic strategy for the treatment of various diseases including genetic diseases, cardiology, neurology and cancer (Pack et al. 2005, 582-587) and involves the transfer of genetic material into target cells (Liu et al. 2019, 42975; Zhang et al. 2021, 12181-12202). Nucleic acids such as messenger RNA (mRNA), small interfering RNAs (siRNAs), DNA plasmids, and micro RNAs (miRNAs) have been used for various gene therapies. However, nucleic acids including DNA, siRNA, mRNA cannot cross the cell membrane on its own. For this reason, they require viral or nonviral delivery systems to enhance its cell permeation. Although viral vectors are widely used due to their high transfection efficiency, safety concerns, their inherently immunogenic nature, causing high immunogenicity and production costs are the main disadvantages of viral vectors (Pack et al. 2005, 582-587). Additional limitations of viral vectors contain low packaging capacity and high cost production (Chen et al. 2022, 484-495). In contrast, non-viral vectors which are polymers, lipids, proteins etc. offer advantages such as easier production and enhanced safety. Lipids and polymers are the most pioneer nonviral vectors due to their safety, flexibility, and high efficiency. Lipids and polymers possess different delivery mechanisms which are the membrane-fusion mechanism and endocytosis-mediated delivery, respectively (Chen et al. 2022, 484-495). Nucleic acids can form complexes with cationic polymers (referred to as polyplexes) or cationic lipids (lipoplexes). Many cationic lipid transfection agents are used for gene delivery, especially in *in vitro* cell assays, and some of these are commercially available (Molla et al. 2020, 852-854). For example, Lipofectamine, which is widely used in *in vitro* studies, is the standard lipid-based commercially available transfection agent (Dakwar et al. 2015, 24322). Lipids are widely used due to their efficiency but have limitations in

reproducibility, stability and toxicity in the production of complexes. Polycations, such as branched poly(ethylenimine) (b-PEI) and poly(2-dimethylamino ethyl methacrylate) (PDMAEMA), are the most common type of nonviral vectors for gene therapy (Witzigmann et al. 2015, 10446). Thanks to the versatility of polymer chemistry, they are amenable to the modifications necessary to provide the functions required for effective gene delivery while maintaining biocompatibility, easy production and robust and stable formulation. As a result, cationic polymers have enormous potential for gene therapy. However, low gene delivery efficiency has limited their clinical application (Pack et al. 2005, 582-587).

2.2. mRNA Delivery

Messenger RNA (mRNA) intercede for the translation of genetic information that comes from DNA into proteins. mRNA has demonstrated significant potential as a safe genetic material for various therapeutic applications, including protein replacement therapy, cancer immunotherapy, vaccines, and gene editing (Kim et al. 2021, 84-87; Yan et al. 2017, 4307-4308). Recently, especially after the pandemic, gene-based therapy become most popular research topic. Even in the treatment of Covid-19, which has affected the world, the mRNA-based Pfizer-BioNTech vaccine has been approved and used as a reliable and effective method (Kim et al. 2021, 84-87; Zhang et al. 2022, 1314). Messenger RNA (mRNA) presents an appealing alternative to other nucleic acids for transfection as it operates directly in the cytoplasm without needing nuclear transfer. Because of different properties, the transfection efficiency and the protein expression rate of mRNA are different than other nucleic acids. Also, there is no risk of integration into the genome. mRNA is rapidly degraded by RNases due to its low stability (Zhang et al. 2022, 1314; Debus et al. 2010, 334-339). Also, mRNA therapeutics can easily degraded via chemical hydrolysis and/or enzymatic action because of their variable phosphodiester bonds. This enzymatic lability provides a limitation for development. mRNA must be protected from these nucleases to ensure its stability (Debus et al. 2010, 334-339). Nevertheless, chemical modification of mRNA has enhanced its stability and capacity of

translation (Chen et al. 2022, 484-495). Also, the movement of mRNA through cell membranes is quite limited due to their intense negative charge and high hydrophilicity.

Each nucleic acid has unique properties. Even though both siRNA and mRNA consist of the same chemical building blocks, they have different modes of action and physicochemical properties. These physicochemical properties consist of size, molecular weight, single stranded or double stranded structure and conformational flexibility. For instance, mRNA is a large and single stranded nucleic acid and the role of mRNA is to carry protein coding information from the genome. Contrary to this, siRNA is a small and double stranded RNA molecules (Chen et al. 2022, 484-495). Single-stranded mRNAs are less stable than double-stranded DNA or siRNAs (Yan et al. 2017, 4307-4308) Protein expression kinetics of mRNA are more consistent than DNA transfection. mRNA molecules reach the cytoplasm to produce functional proteins. Unlike DNA-based gene therapy, these molecules do not reguire entry into the nucleus. Such differences require uniqueness in the carrier molecules developed. Because a vector that provides one tye of nucleic acids with high efficiency and stability may not carry another molecule with the same efficiency (Chen et al. 2022, 484-495). In summary, the mRNA platform offers several benefits over other nucleic acid based therapeutics as rapid protein expression, potential to avoid nuclear localization, low mutagenesis risk, easier and flexible design, cost-effective preparation, low biosafety risk. On the other hand, mRNA presents limitations for being used as a gene-based therapeutic. These limitations include large size, immunostimulatory effects, low cell uptake, low stability and poor bioavailability (Chen et al. 2022, 484-495; Islam et al. 2015, 1519-1530). Therefore, efficient and safe vectors are required to protect mRNA from degradation, minimize immunostimulatory effets, enhance cell uptake and to achieve efficient delivery of mRNA molecules to the desired therapeutic site (Chen et al. 2022, 484-495; Islam et al. 2015, 1519-1530). Recently, variety of mRNA based delivery nanoplatforms have been developed. The development process include variousd stages such as safety evaluation, determination of administration routes, and preparation technology as shown in Figure 2.1 (Zhang et al. 2022, 1314). To develop efficient and safe delivery technology, it is necessary to improve existing mRNA-based delivery nanoplatforms such as lipid nanoparticles, liposomes, polymeric nanoparticles, hybrid nanoparticles and nanoemulsions.

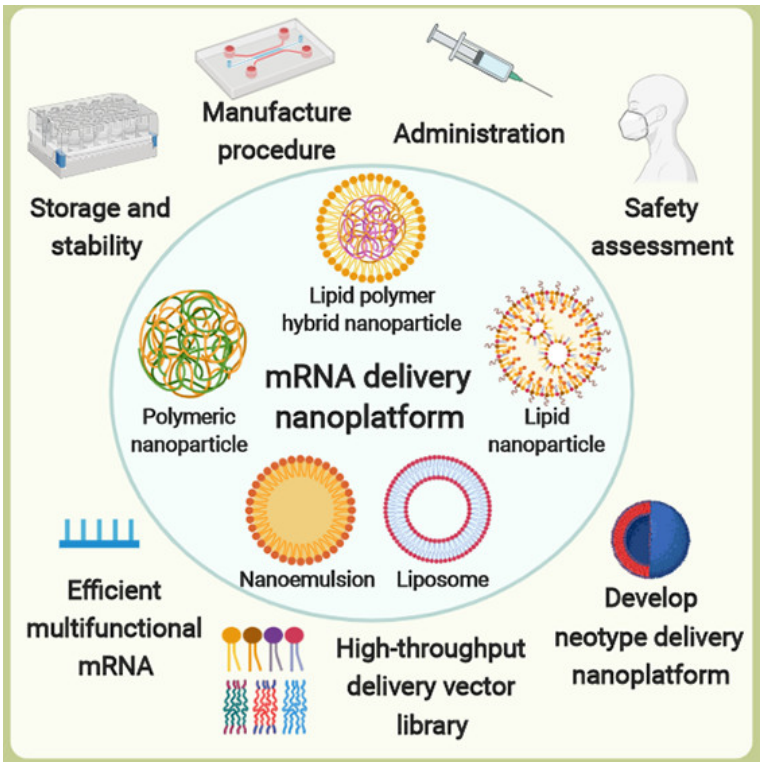

Figure 2.1. General scheme of mRNA delivery system development (Zhang et al. 2022, 1314).

Nanovectors, such as lipid nanoparticles and polymeric nanoparticles, play a crucial role in safe and stable delivery of mRNA. Lipid-based nanoparticles (LNPs) are currently used in clinical trials (Yan et al. 2017, 4307-4308). They are mostly preferred because of their high transfection efficiency and biocompatibility, although they face challenges such as storage instability and issues related to immunogenicity (Zhang et al. 2022, 1314-1315).

2.3. Cationic Polymers for mRNA Delivery

Many types of polymeric nanoparticles have been designed for delivery of genes such as DNA, siRNA, mRNA (Islam et al. 2015, 1519-1530). Polymer vectors offer several advantages, including versatile structural diversity, the ability to make surface

modifications with other materials, low toxicity and immunogenicity. Polymers used for gene delivery can have linear, branched, or dendritic structures. Due to the flexibility of polymer chemistry, they can potentially provide multiple functions necessary for efficient gene delivery while maintaining biocompatibility, ease of manufacturing, and robust, stable formulations. Consequently, polymers hold significant potential for human gene therapy. However, their clinical application has been limited by poor gene transfer efficiency. Especially cationic polymers are used in nucleic acid delivery. Cationic polymers can form complexes with nucleic acids via electrostatic interactions between the negative phosphates from the mRNA and positive charges displayed on the cationic polymers as shown in Figure 2.2 (Pack et al. 2005, 582-587). The compact structures (polyplexes) form spontaneously. The structure and morphology of polyplexes may be kinetically controlled and the polyplex stability depends on the polymer structure and N/P ratio. Favourable electrostatic interaction cabability mediates the binding strength between the negatively charge nucleic acids as mRNA (Islam et al. 2015, 1519-1530). The binding strength provided by electrostatic attraction between mRNA and polymer, which is increased by modifying the charge and size of the polymers used, is an important factor in mRNA expression efficiency.

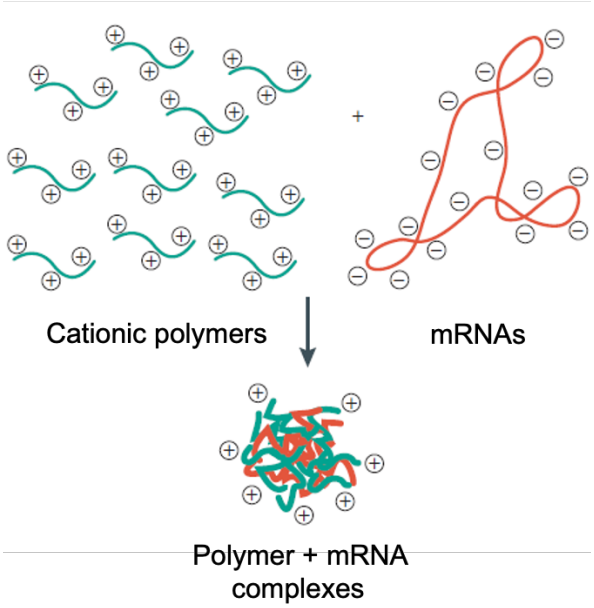

Figure 2.2. Formation of polplexes via electrostatic interaction between cationic polymer and mRNA (Pack et al. 2005, 582).

In studies with polyethyleneimine (PEI) to observe the effect of molecular weight, it was found that PEI with higher MW had better endosmotic activity. In addition, *in vitro* cytotoxicity decreased with decreasing molecular weights. Among polymeric carriers for gene delivery, polyethyleneimine (PEI) become a gold standard for nucleic acid transfection due to high transfection efficiency (Pack et al. 2005, 582-587). PEI which consists of high amount of amines has a strong proton sponge capacity. This property can be attributed to its buffering capacity and creates a high positive charge density under physiological and acidic conditions. Thanks to this feature, it creates strong electrostatic interactions with nucleic acids under physiological conditions. It also facilitates the escape of nucleic acids from the endosome via the proton-sponge effect. Despite all these advantages, it creates limitations in clinical applications due to its high toxicity (Chen et al. 2022, 484-495). Due to its high cationic charge density and flexible structure, PEI can be complex with negatively charged nucleic acid through electrostatic interactions.

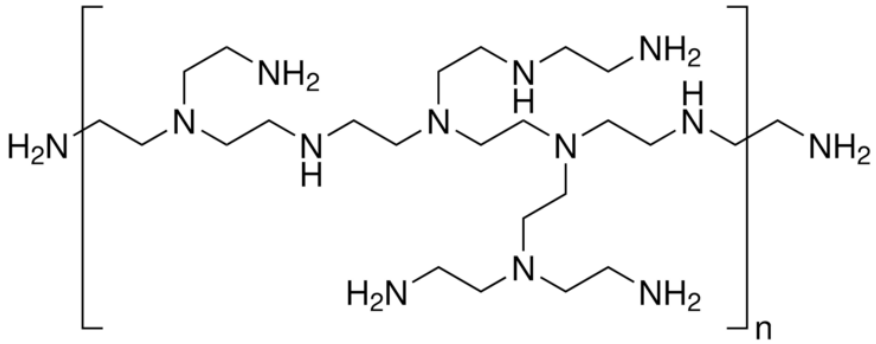

Figure 2.3. Chemical structure of branched PEI (Polyethylenimine, Branched, Merck).

Although PEI (25 kD), which is shown in Figure 2.3, is known for its high transfection efficiency *in vitro* experiments, it shows a high cytotoxicity effect. The toxicity of PEI is related to its cationic surface groups. And this may increase with the molecular weight of the polymers. The positive charges on the surface of PEI help it to interact with the cell membrane and proteins through electrostatic interaction. This can also be observed by dendrimer-based cationic polymers. The same effect is observed in polyamidoamine (PAMAM) dendrimers with amine-terminated groups, which have a similar cationic structure to PEI. In order to optimize the balance between toxicity and

efficacy of cationic polymers, modifications are made to the polymer structures. For example, combinations of low molecular weight PEI (600 kD) with structures such as poly(ethylene glycol) (PEG) and lipids have been observed to increase biocompatibility and efficiency. PEI-based polymers, which have high application potential in gene delivery, have limitations due to their high toxicity due to strong electrostatic interactions with cell membranes and extracellular matrix (Pack et al. 2005, 582-587). Many of the efficient cationic polymer vectors contain repeating units of the diaminoethane (DET) motif, known for its two-step protonation property. This property grants the polymer a high proton sponge capacity and membrane destabilization ability during endosomal acidification, leading to high transfection efficiency. At physiological pH, the DET motif is partially protonated, but it becomes fully protonated at the acidic pH of the endosome. Polymers with protonable groups at endolysosomal pH can escape from the endosome via the proton sponge theory which is illustrated in Figure 2.4 (Islam et al. 2015, 1519-1530). Polyplexes initially localize within endocytic vesicles. These vesicles then fuse with sorting endosomes, from which the internalized material can be transported back to the membrane and expelled from the cell via exocytosis. Once released from endosomal compartments, polyplexes must traverse the cytoplasm to reach the nucleus. However, the cytoplasm is densely packed with proteins, microtubules, and other organelles, which can impede polyplex movement. Positively charged polyplexes can move along microtubules. Endolysosomes are acidified by the action of an ATPase enzyme that actively transports protons from the cytosol into the vesicle. These polymers, therefore, undergo large changes in protonation during endocytic trafficking. It has been proposed that proton-sponge polymers prevent acidification of endocytic vesicles, causing the ATPase to transport more protons to reach the desired pH. The accumulation of protons in the vesicle must be balanced by an influx of counter ions. The increased ion concentration ultimately causes osmotic swelling and rupture of the endosome membrane, which releases the polyplexes into the cytosol (Pack et al. 2005, 582-587). The buffering capacity of these materials causes an influx of protons and chloride ions, resulting in water diffusion and osmotic swelling. Consequently, the endosome membrane disrupts, releasing the nanoparticles into the cell cytosol.

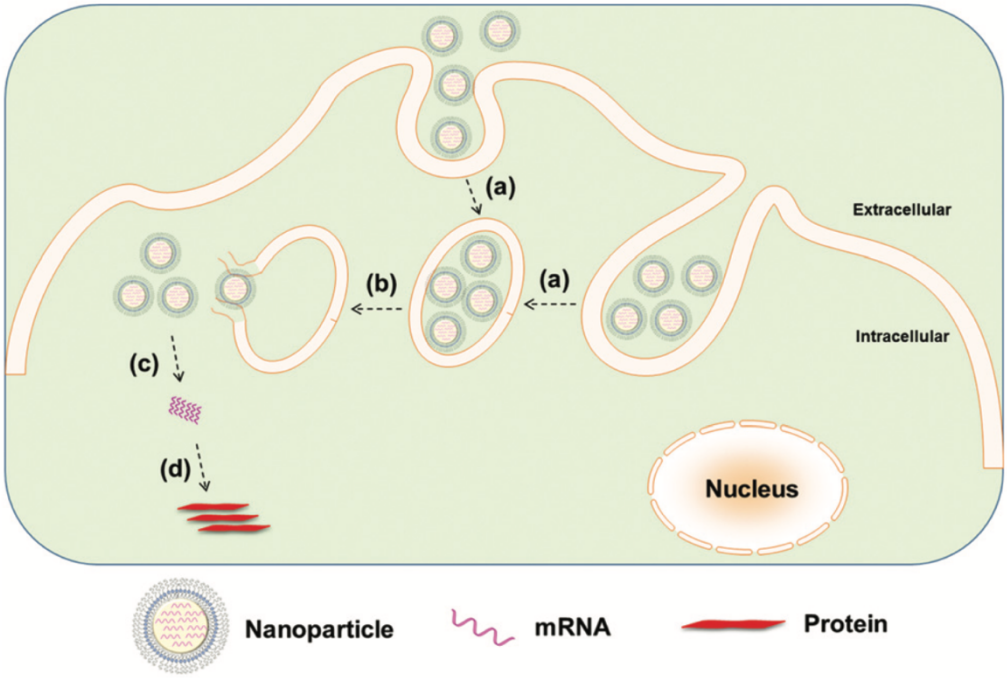

Figure 2.4. Endosomal escape ability of nanoparticle based mRNA delivery (Islam et al. 2015, 1524).

2.4. Zebrafish as an In Vivo Model

New vectors responsible for the delivery of nucleic acids to target cells are still being developed to meet clinical needs. To enable the clinical use of newly developed vectors, various animal models are employed to evaluate cruical parameters such as biodistribution, toxicity and efficacy in preclinical studies. Although rodents (mice and rats) are commonly preferred due to their anatomical and genomic similarities to humans, they have disadvantages, including high maintenance and development costs and small progeny, which hinder rapid and large number trials (Table 2.1). To overcome these limitations, zebrafish *(Danio rerio*) has recently been widely adopted as a next-generation *in vivo* animal model.

Zebrafish was initially introduced by Streisinger and colleagues in 1980s. High level of genome structure (~70%) is shared between zebrafish and human genes (Martinez-Lopez et al. 2021, 7). And also, zebrafish possess metabolic characteristics similar to humans. Zebrafish embryos have yolk sac like human embryos. Yolk consists

of proteins, micronutrients, and lipids (cholesterol, phosphatidylcholine, and triglycerides) that can sustain metabolic function, and growth until the onset of exogenous feeding, mediate cell signaling, and also provide building blocks of plasma and cell membranes (Sant, Timme-Laragy. 2018, 125-130). Zebrafish embryos have an innate immune system at the larval stage, similar to mammals, and an adaptive immune system after four to six weeks of development. Due to their advantages over other animal models, such as embryo transparency, high fertility in a short production time, easy production and maintenance conditions, easy handling due to their small size, a short life cycle that allows main organs to develop within 48 hours post-fertilization (hpf), low cost, and a fully sequenced genome with controlled gene expression, zebrafish are used as models in various research fields. Although analyzing both bacteria and nanoparticle mediated drug delivery in real-time in animal models such as mice is complicated, the zebrafish model allows visualization in real-time due to its optical transparency property. Thanks to these unique properties, Fenaroli et al. investigated to visualize the effect of fluorescent mycobacteria and nanoparticles administered by different routes (injection, orally, etc.) in real-time in living vertebrate zebrafish embryos (Fenaroli et al. 2014, 7014-7015).

Molla et al study evaluated the effect of lipidoids on siRNA delivery for stability and cytotoxicity *in vitro*, first. Then best-performing lipidoid was selected and this one toxicity and transfection efficiency compared with Lipofectamine, which is a commercially available transfection reagent, was investigated in a zebrafish *in vivo* model (Molla et al 2020, 852-854). Models used to study the physiological dynamics of the heart in research must have highly specialized imaging and data processing pipelines. Zebrafish is a widely used predictive model especially on cardiovascular development (Goudy et al. 2019, 1-3). Hu et al. investigated the cardiovascular toxicity evaluation of poly(ethyleneimine) cationic polymers with different molecular weights in a zebrafish model (Hu et al. 2015, 768-769).

While their simple structures often provide advantages, they also lead to certain limitations. Due to their lack of complexity compared to humans, zebrafish models need to be supported by other *in vivo* models. Hence, they are described as intermediate models. Toxicity evaluations conducted on zebrafish embryos have shown a predictability level of 65-85% according to the European Centre for Validation of Alternative Methods guideline. Consequently, zebrafish can be used as a pioneer model in future animal experiments, potentially reducing the number of animals required in subsequent stages (Rizzo et al. 2013, 3919-3923).

When toxic substances are used in zebrafish embryos, teratogenic malformations, also known as teratogenesis, can occur, leading to structural or developmental abnormalities. The substances causing this effect are called teratogens, and the resulting abnormalities in body form and shape are referred to as malformations. The embryonic stage affects vulnerability to teratogenic malformations. The most critical and sensitive period of embryonic development is the 24-hour post-fertilization stage, during which organogenesis occurs. At this stage, the rapid differentiation of organs takes place. The high rate of cell proliferation makes the embryo susceptible to teratogenic factors (Rizzo et al. 2013, 3919-3923).

Tablo 2.1. Comparison of *in vitro* cell models with *in vivo* models such as zebrafish embryos and rodent models (Bondue et al. 2023, 3).

***In Vivo* Models**	**Zebrafish Larval Models**	**Rodent Models**
Low maintenance cost	Low maintenance cost	High maintenance cost
Simplified	Moderate difficulty	High difficulty
Short timeframe	Short timeframe	Long-term experiments
Poor translatability	Moderate translatability	High translatability
High flexibility	Moderate flexibility	Low flexibility
Unrealistic cellular morphology and interactions	Genetic similarity to humans	Genetic similarity to humans
High throughput	High throughput	Low throughput
Easy genetic modulation	Easy genetic modulation	Complex genetic modulation
Rapid genetic rescue	Rapid genetic rescue	More complex genetic rescue
Naked or packaged mRNA	Naked or packaged mRNA	Preferably packaged mRNA
Direct transfection of all cells	Ubiquitous expression (one-cell stage injection)	Restricted expression (vehicle dependent)
Effectively of mRNA-based therapy	Effectivity+delivery of mRNA-based therapy	Effectivity+delivery of mRNA-based therapy
Low to moderate ethical considerations	Low ethical considerations (<120 hpf in Europe)	High ethical considerations

CHAPTER 3

MATERIALS AND METHODS

3.1. Materials

The block copolymer of oligo(ethylene glycol) methacrylate (OEGMA) and 2-((aminoethyl)amino)ethyl methacrylate (AEAEMA) monomers, $P(OEGMA)_{42}$-b-$P(AEAEMA)_{48}$ synthesized according to the protocol reported elsewhere (Zelcak 2021, 36-44) was used throughout this study. The commercial transfection agent Lipofectamine 3000 (Thermo Fisher) and branched poly(ethyleneimine) (PEI) (MW=25kDA) (Sigma-Aldrich, MO, United States of America), were used as positive controls in *in vivo* experiments.

The GFP mRNA (MW= 331,77 kDA, 1000 bases) and zebrafish embryos were supplied by Professor Dr. Hatice Güneş Özhan from the Izmir Biomedicine and Genome Center (IBG). Zebrafish breeding and raising were carried out in special rooms and under controlled conditions according to the guidelines of IBG. All animal experiments were performed in a procedure approved by the IBG Animal Experiments Local Ethics Committee (IBG-AELEC). Two different zebrafish models were used which were AB strain wild-type (wt) and Casper type (lacks melanocytes and iridophores). Embryos were incubated in Pronase (Sigma-Aldrich, MO, United States) solution for dechorionation procedure. Phenol Red (Sigma-Aldrich, MO, United States of America) was used in the initial microinjection experiments. 10 mg/ml of Tricaine (MilliporeSigma, MA, United States) was used for anesthesia. Borosilicate glass capillaries (4 inches, OD 1.0 mm, World Precision Instruments, FL, United States) were used as injection needles. E3 medium (NaCl, KCl, $CaCl_2 \cdot 2H_2O$, and $MgCl_2 \cdot 6H_2O$ and pH 7.2) was used as growth medium for embryos. 4′,6-diamidino-2-phenylindole (DAPI; 4083S, Cell Signaling Technology, MA, United States of America) was used for nuclear staining. GFP (D5.1) Rabbit mAb (2956s) from Cell Signaling Technologies (Danvers, Massachusetts, USA)

was used for the primary antibody. PBDX_GS blocking solution consisted of 10% bovine serum albumin (GoldBio), 15 µL/1 mL goat serum, 0.3% Triton-X (Bioshop), and 1% DMSO (Fisher). Thermo Fisher Dulbecco's Phosphate Buffered Saline (PBS) adjusted at pH 6.5 was used for polyplex preparation.

Agarose LE (A-201-100, GoldBio, U.S.) was used for agarose gel preparation. TAE buffer consisted of Acetic Acid (Glacial) (Merck, Germany), EDTA Disodium Salt Dihydrate (Amresco, U.S.), TRIS (Amresco, U.S.). SafeView Classic G108 (Applied Biological Materials (ABM), Canada) was used for nucleic acid stain for the visualization of RNA in agarose. DNA Gel Loading Dye (6X) from Thermo Fisher was used.

3.2. Instruments

3.2.1. Micromanipulation unit

High-precision injections of zebrafish embryos and adults were performed in the micromanipulation unit at İBG. Centralized filtration multilink type zebrafish aquarium system (Techniplast ZebTEC “Active Blue” Technology) were used. Micromanipulation unit consist of a Borosilicate glass capillary (World Precision Instrument), Flaming/Brown Micropipette Puller (Sutter Instrument), and PV820/PV830 Pneumatic Picopump (World Precision Instrument).

3.2.2. Agarose Gel Electrophoresis

Horizontal Gel Electrophoresis System (Biorad Wide Mini-Sub Cell GT) was used. BIO-VISION+1500/20M X-Press (Vilber Lourmat, Germany) gel imaging system was used to evaluate the characterization of polyplexes. BioRad PowerPac Basic 300 V (Bio-Rad, California, United States) was used for power supply.

3.2.3. Stereo Microscopy

To evaluate the toxic effect of polymers and the mRNA transfection efficiency of the control groups and the block copolymer was first observed using a stereo microscope. Olympus SZX16-ILLB stereomicroscope (Olympus Corporation, Japan) with equipped with a trinocular tube and Olympus DP series digital camera were used. DP series camera offer high sensitivity fluorescence imaging. The images were visualized using the Olympus cellSens software.

3.2.4. Fluorescence Microscopy

Immunostaining was performed on samples with high transfection efficiency. Samples were visualized using Olympus BX61 fluorescence microscopy (Olympus Corporation, Japan) on the coverslip. Images were analyzed using ZEN software.

3.2.5. Confocal Microscopy

Immunostaining was performed on the fixed samples to visualize transfection efficiency in more detail and to enable data analysis. The samples were analyzed at 25X and 63X objective lenses using the z-stack function and the DAPI and FITC channels of the confocal microscope on the coverslip. Zeiss LSM880 confocal microscope (Carl Zeiss AG, Jena, Germany) at IBG and Leica STELLARIS DLS digital light sheet microscope (Leica Microsystems, Germany) at Ege University were used. Image J and ZEN tools were used for data analysis of the images obtained as a result of visualization.

3.3. Methods

3.3.1. Polyplexes Formation

All polymers ($P(OEGMA)_{42}$-b-$P(AEAEMA)_{48}$ and branched PEI (b-PEI) were complexed with mRNA (2000 ng) in PBS (at pH 6.5) to prepare polyplex formulations at varying N/P ratios. Stock solutions (20 mg/ml) of the $P(OEGMA)_{42}$-b-$P(AEAEMA)_{48}$ (29 kDA, PDI= 1.03) and b-PEI (25 kDA) were prepared by dissolving the respective polymer in PBS (at pH 6.5). From the prepared $P(OEGMA)_{42}$-b-$P(AEAEMA)_{48}$ stock solution (20 mg/ml), 0.015 mg (0.75 µL), 0.030 mg (1.50 µL), and 0.045 mg (2.25 µL) were added into Eppendorf tubes to prepare polyplexes with N/P 3.6, N/P 7.3, and N/P 10.9 ratios, respectively (Table 3.1). Then 2.25 µL, 1.5 µL, and 0.75 µL of PBS (at pH 6.5) were added sequentially onto each polymer to make the total volume of each tube was 5 µL. Lastly, mRNA (2000 ng, 2 µL) was added, and all complex was mixed with a micropipette. The prepared polyplexes were kept at room temperature for 25 minutes.

For PEI, which was used as a golden standard polymer, toxicity experiments were performed using a fixed amount of mRNA (2000 ng) at different N/P ratios. Using the same method, 0.010 mg, 0.021 mg, and 0.041 mg of PEI (20 mg/ml) stock solution were added to Eppendorf tubes for N/P 25, 50, and 100, respectively (Table 3.1), and the required amount of PBS (at pH 6.5) was added onto each tube to make the total volume of each tube was 5 µL. Finally, mRNA (2000 ng, 2 µL) was added. The final polyplex solutions were incubated at room temperature for 25 minutes before analysis.

Table 3.1. Preparation of Polyplexes.

Total mRNA amount (2000 ng)			
$P(OEGMA)_{42}$-b-$P(AEAEMA)_{48}$		**b-PEI (25 kDA)**	
N/P	Stock Solution (20 mg/ml)	N/P	Stock Solution (20 mg/ml)
3.6	0.015 mg	25	0.010 mg
7.3	0.030 mg	50	0.021 mg
10.9	0.045 mg	100	0.041 mg

In accordance with the manufacturer's protocol (Lipofectamine^{TM} 3000 Reagent Protocol Protocol Outline, 2016), Lipofectamine (0.4 µL) was complexed with mRNA (2000 ng) in PBS (at pH 6.5). The total volume of the final solution was 5 µL. This complex solution was kept at room temperature for 25 minutes. The same complexation protocol was used to prepare complexes of Lipofectamine and mRNA for optimizing transfection experiments using zebrafish. In these optimization experiments an mRNA dose of 1000 ng was used. The quantity of other reagents was used accordingly.

3.3.2. Characterization of Polyplexes

The characterization of polyplexes formed with $P(OEGMA)_{42}$-b-$P(AEAEMA)_{48}$/mRNA and PEI/mRNA was performed using agarose gel electrophoresis. For block copolymer polyplexes which were formed with a fixed amount of mRNA (2000 ng), and varying polymer amounts to yield varying N/P ratios (3.6, 7.3, and 10.9) were mixed with gel loading dye (1 µl) and loaded onto a 1% agarose gel. Also, for PEI/mRNA complexes, polyplexes formed with both 1000 ng mRNA at N/P 100 and 2000 ng mRNA at N/P 50 were mixed with gel loading dye (1 µl) and loaded onto a 1% agarose gel. Polymer-mRNA complexes, marker and naked mRNA were run on agarose gel in TAE (1x) buffer at 90 V for 40 minutes. EtBr was not used during these steps due to its toxic effect. Instead of EtBr, SafeView Classic G108 (ABM, Canada) was preferred. The gel was visualized using a BIO-VISION+1500/20M X-Press (Vilber Lourmat, Germany) imaging system and analyzed under UV light.

3.3.3. Breeding

Two different zebrafish models (AB wild-type (wt) and Casper type) were used. In the IBG Vivarium, lighting (12 hour light and 12 hour dark cycle) and heating systems (28ºC) were automated to simulate the natural environment and to provide the necessary environmental conditions as defined by the IBG Animal Care and Use Committee.

Aquarium tanks with automatic filtration systems were available in the vivarium. Adult zebrafish are transferred to breeding tanks with removable sieves gear to the number of male fish outnumber the number of females. This apparatus holds the eggs in a separate section from the fishes. Thus, the fish don't eat the eggs. Tanks are kept overnight. After spawn, eggs are collected into petri dishes that include E3 medium with a strainer.

3.3.4. Microinjection

Microinjection was performed according to the embryonic stage to be used after fertilization (0 hpf, 24 hpf, 48 hpf). Before the injection, the chorions of the embryos were removed using physical or chemical methods. Pronase solution was used to enzymatically digest the chorion. For chemical dechorionation, Pronase (500 µL, 10 mg/ml) was added to E3 medium (50 mL). The embryos in the plate were kept in the incubator (28ºC) for approximately 10 minutes. Then, they were separated from their chorions by pipetting with a Pasteur pipette. For the physical method, a tear was made between the embryo and the chorion with the help of forceps and the chorion was broken and separated. Care was taken not to damage the embryos at the young embryonic stage because they were fragile. For 48 hpf embryos, the chorions were physically removed using a tweezer under a microscope. Tricaine (10 mg/ml) was used for narcosis before injection. 10-15 drops of Tricaine (10 mg/ml) were added to the embryos in the plate and kept waiting. The prepared embryos were then transferred to injection cups prepared with agarose gel and aligned along the wells of the gel. Sufficient amount of E3 medium was added to the embryos to prevent them from drying out. The mixtures were loaded in borosilicate glass needles (4 inches, OD 1.0 mm, World Precision Instruments, FL, United States) using a 20 µl microloader pipette, taking care to avoid air bubbles. Then, the tip of the needle inserted into the micromanipulator was broken with a tweezer. This step allows the needle tip to become sharper and the injection to be easier. The prepared polyplex mixtures and control groups were injected into different parts of the zebrafish embryos (caudal vein, trunk, pericardial cavity) using pressure from micromanipulator. The injected embryos were then transferred to petri dishes containing E3 medium and incubated overnight at

28°C. Since it was determined that phenol red dye might have increased the toxic effect, injections were performed without using any dye.

3.3.5. Fixation

For the fixation process consisting of two stages, firstly, the embryos that had been in the petri dish for 24 hours were transferred into a 2 µl Eppendorf tube. E3 medium in the Eppendorf tubes was removed with the help of a micropipette. Then approximately 2 µl paraformaldehyde (PFA) (4%) was added to the embryos. It was kept at +4°C for 24 hours.

At the second step, embryos that were kept in PFA (4%) were removed from the cold environment at +4°C. PFA (4%) on the embryos was removed with a micropipette in the fume cupboard. Washing was performed with PBS (2 µl) at pH 6.5. After the washing step, PBS (at pH 6.5) was removed, and cold methanol (100%) (2 µl) was added. Eppendorf tubes were stored horizontally at -20°C.

3.3.6 Immunostaining

Immunofluorescence staining method include a few steps which are permeabilization, primary and secondary antibody incubation, washing, fixation and storage in the mounting media. Embryos initially stored in MetOH were rehydrated with decreasing concentration of MetOH (75%, 50%, 25% MetOH diluted in PBS/0.05% Tween) (2 µL) and then washed 4 times in PBS/0.05% Tween (2 µL) and once in water (2 µL) for 5 minutes each. The water was replaced with cold acetone (2 µL) and the embryos were incubated at -20 °C for 7 minutes. Then the embryos were washed twice in PBS/0.05% Tween (2 µL) for 10 minutes. The samples were incubated with blocking solution (PBDX_GS) (500 µL) in well plate for 1 hour at room temperature. The blocking solution was removed and the primary antibody dilution (1 µL), which is anti-GFP, was

added on of PBDX_GS blocking solution (250 µL). The mixture was incubated for 1h at room temperature and kept at 4 °C overnight.

The primary antibody was removed, and the sample was washed twice for ten minutes in PBS/0.05% Tween (250 µL). Washing was repeated six times for a period of 30 minutes, each time using a solution of phosphate-buffered saline (PBS) and 0.05% Tween (250 µL). The PBS/0.05% Tween solution was then removed. The secondary antibody dilution (1 µL), along with 1 µL of DAPI (50 µg/mL) diluted in PBDX_GS (250 µL) was added and incubated for one hour at room temperature and then kept at 4 °C overnight.

The secondary antibody dilution was removed, and the samples were washed four times for 15 minutes in PBS/0.05% Tween (250 µL). The samples were fixed in 4% paraformaldehyde (PFA) (250 µL) at room temperature for 20 minutes. Subsequently, the samples were washed once in PBS/0.05% Tween (250 µL) for a period of 5 minutes. Then, the PBS/0.05% Tween solution was removed and replaced with glycerol (2 µL) in each microcentrifuge tube. The embryos were stored horizontally in the dark at 4°C until mounting.

3.3.7. Mounting & Imaging

After 24 hours of incubation, the embryos were first observed under stereo microscope. Tricaine (10mg/ml) was used as narcosis to limit the movements of the zebrafish during the imaging process. Imaging was then performed using the cellSens program. Samples with high radiation potential were fixed between two coverslips after fixation and immunostaining. For this, a drop of glycerol was placed on the first coverslip under a microscope and protected from light. A few of the embryos to be visualized were placed on it. After correcting the position of the embryos via the microscope, they were placed on the second coverslip. The embryos between the two coverslips were fixed with glue. They were kept at 4°C and protected from light until the image was taken. Images of the embryos were taken at 25X and 63X using the DAPI and FITC channels of the confocal microscope. After confocal microscopy imaging, image analysis was performed

using ZEN software. In addition, the Image J program was used to perform quantitative analysis.

CHAPTER 4

RESULTS AND DISCUSSION

4.1. Optimization of Transfection Experiments using Zebrafish Model

The optimal conditions for *in vivo* transfection experiments using the zebrafish model have been first determined. In this context, various parameters were separately evaluated, including zebrafish type (Casper type and/or AB type), embryonic developmental stage (0 hpf, 24 hpf, 48 hpf), injection site (pericardial cavity, trunk, circulation), mRNA administration method, and mRNA dose using Lipofectamine as a transfection agent.

Two different mRNA administration methods were first investigated to observe the transfection. These methods included adding Lipofectamine-mRNA (1000 ng) complex to the medium in the well-plate and microinjection using naked embryo and naked mRNA in PBS as a control group. The same amount of mRNA (1000 ng) was used for all sets of experiments. For the treatment method, zebrafish embryos at 24 hpf were placed in a 24 well-plate with 10 eggs/well. The total volume in a well was set to 250 µl and 5% of the total volume was set to be Lipofectamine/mRNA complex, naked mRNA (1000 ng) with PBS (at pH 6.5) and naked embryo solution in PBS (at pH 6.5). The GFP expression was investigated 24 h after the administration of Lipofectamine/mRNA complex treatment at 24 hpf (hours post fertilization) zebrafish embryos via stereo microscope (SZX16, Olympus) (Figure 4.1A). As it can be seen from the images, there was no transfection of mRNA in the experiments where Lipofectamine/mRNA complex and naked mRNA were added to the medium. In the second set of experiments, Lipofectamine/mRNA (1000 ng) complex in PBS (at pH 6.5) and naked mRNA (1000 ng) in PBS (at pH 6.5) were injected into the embryos pericardial cavity. During these experiments, to observe the onset of expression post-treatment/injection, imaging was performed at different time intervals for 24 hours after introducing GFP mRNA. Embryos

were observed using a stereo microscope (SZX16, Olympus). It was observed that the expression became apparent between 16 and 24 hours post-injection into the pericardial cavity for the Lipofectamine/mRNA (1000 ng) complex in PBS (at pH 6.5) (Figure 4.1B). Hence, GFP expression was observed in experiments where the microinjection method was utilized with an mRNA-lipofectamine complex (mRNA dose of 1000 ng). The results also indicated that the protein expression was detectable between 16 and 24 hours. In both methods, mRNA expression wasn't observed for naked mRNA in PBS solution and naked embryos. Since no fluorescence was observed with the direct addition method under the stereo microscope, the microinjection method was preferred for the rest of the study according to the results of the lipofectamine/mRNA complex.

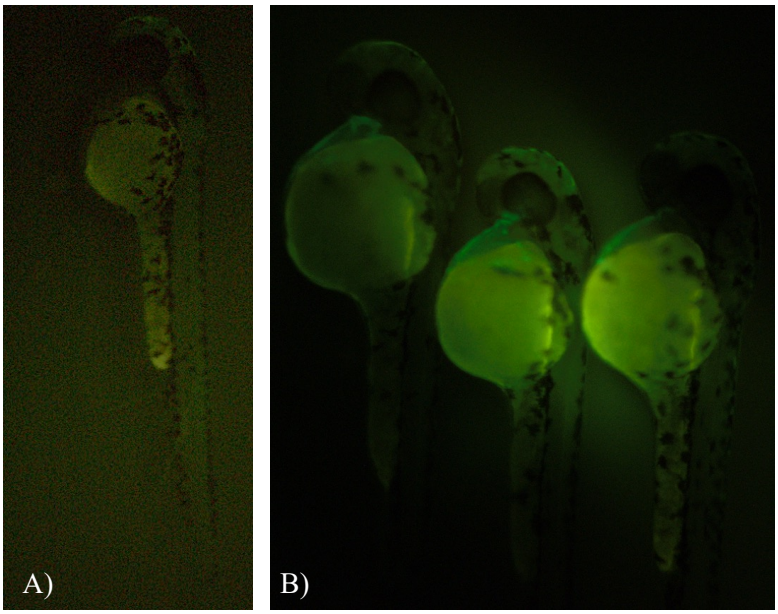

Figure 4.1. Stereo microscope (SZX16, Olympus) results of GFP expression, 24 hours after the administration of Lipofectamine- mRNA (1000 ng) complexes via two different methods; A) direct addition to the medium and B) injection into the pericardial space of 24 hpf zebrafish embryos.

The type of zebrafish was investigated at the next step. The AB and Casper type zebrafish were administered with GFP mRNA-Lipofectamine complex containing 1000 ng mRNA via microinjection method. It was observed that visual blight was caused by

AB type zebrafish embryos during imaging (Figure 4.2A). On the other hand, Casper type zebrafish provided clearer images because of their transparency and thus were used in subsequent experiments (Figure 4.2B).

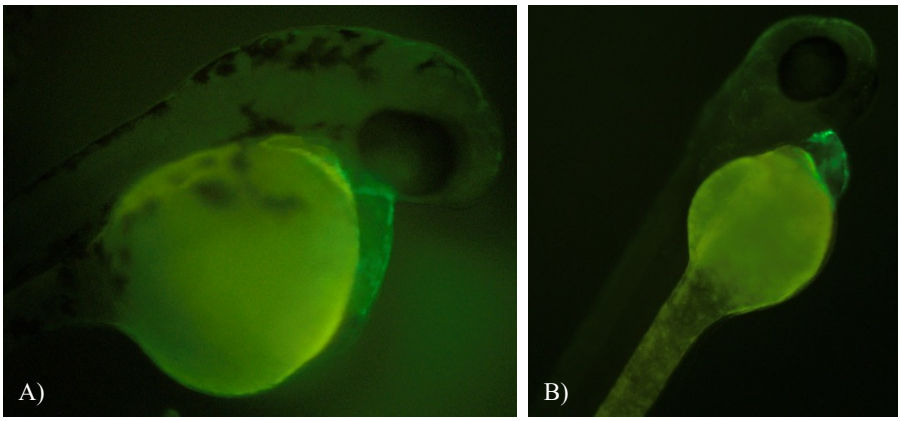

Figure 4.2. Investigation of mRNA transfection on different types of zebrafish: (A) AB type, and (B) Casper type zebrafish after administration of eGFP mRNA (1000 ng)-Lipofectamine complexes via microinjection. The images were taken using a stereo microscope (SZX16, Olympus).

Subsequently, to observe the effect of the embryonic stage on the injection, Casper type zebrafish embryos at 0 hpf (hours post fertilization), 24 hpf, and 48 hpf were injected separately with naked mRNA (1000 ng). The presence of the chorion has limited the use of 0 hpf and 24 hpf embryos. Because of the damage caused to embryos by the physical and chemical methods used for dechorionation and the increased sensitivity of zebrafish embryos at earlier stages, it was found that using 48 hpf embryos, the stage at which they naturally separate from the chorion, was more ideal. Additionally, the use of 48 hpf embryos helped to serve as a precursor for future experiments planned with adult zebrafish, as this stage is the closest to the adult zebrafish model.

At the next step, transfection experiments were conducted in three different regions (pericardial cavity, trunk, and circulation) of Casper embryos at 48 hpf to observe the effect of injection site on the mRNA transfection. The Lipofectamine-mRNA (1000 ng) complex formulations were injected into different sites (pericardial cavity, trunk, and circulation) of 48 hpf Casper type zebrafish embryos. 24 hours after the injection the

stereo microscope results indicated that the pericardial cavity, which allows for relatively easier injections, was identified as the ideal region due to its high transfection efficiency compared to other sites (Figure 4.3).

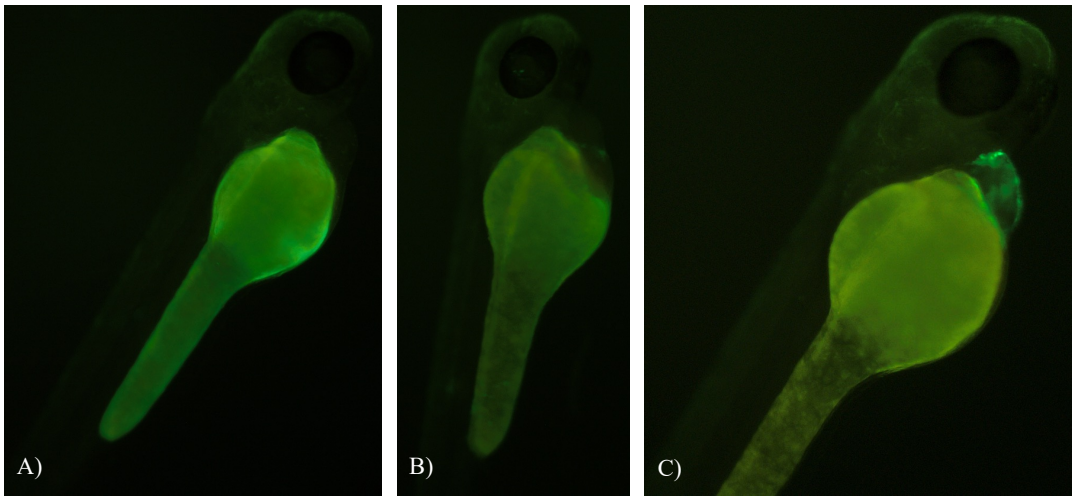

Figure 4.3. Stereo microscope (SZX16, Olympus) images of 24 hours after the microinjection of the Lipofectamine- mRNA complexes (1000 ng mRNA) at three different sites of Casper embryos at 48 hpf (A) circulation; B) trunk; C) pericardial cavity).

In order to support the results obtained via stereo microscopy, a more detailed analysis was performed using a confocal microscope. Lipofectamine-mRNA (1000 ng) complexes were injected into the pericardial cavity region of 48 hpf embryos and after immobilization, sections were visualized from different parts of the fish as shown in Figure 4.4. Injections into the trunk (Figure 4.5) and caudal vein (Figure 4.6) regions were also performed and visualized using the same methods. The pericardial cavity was preferred as the injection site due to better fluorescence visualization according to the results.

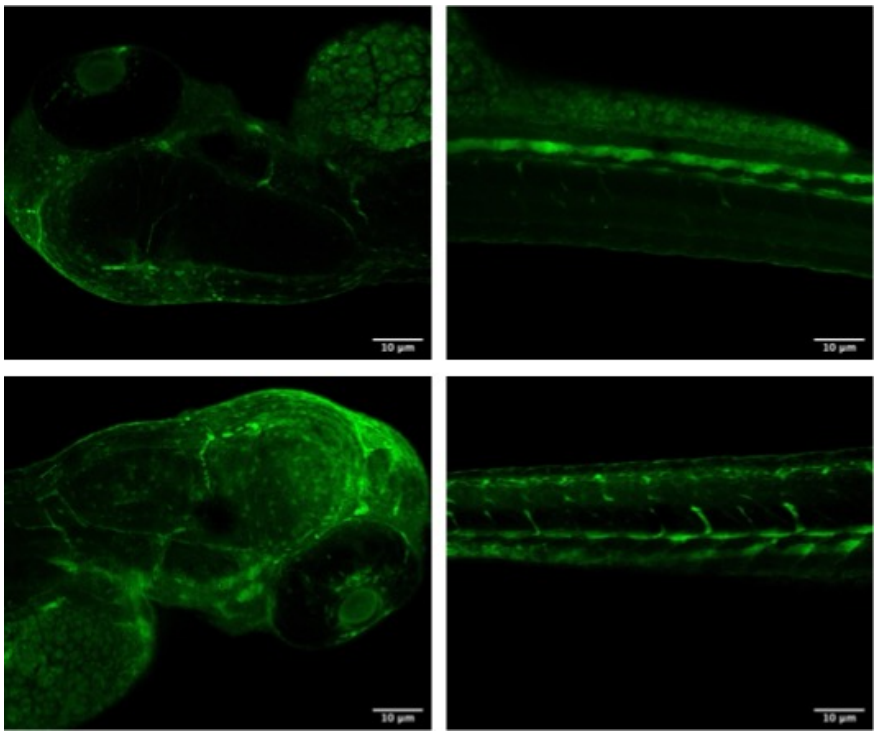

Figure 4.4. Confocal microscope images of 24 hours after the microinjection of Lipofectamine-mRNA complexes (1000 ng mRNA) at the pericardial cavity of Casper embryos at 48 hpf.

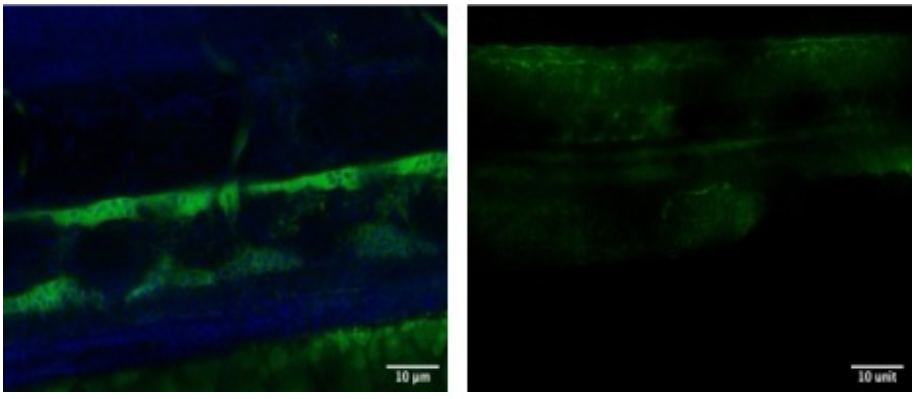

Figure 4.5. Confocal microscope images of 24 hours after the microinjection of Lipofectamine-mRNA complexes (1000 ng mRNA) at the trunk of Casper embryos at 48 hpf.

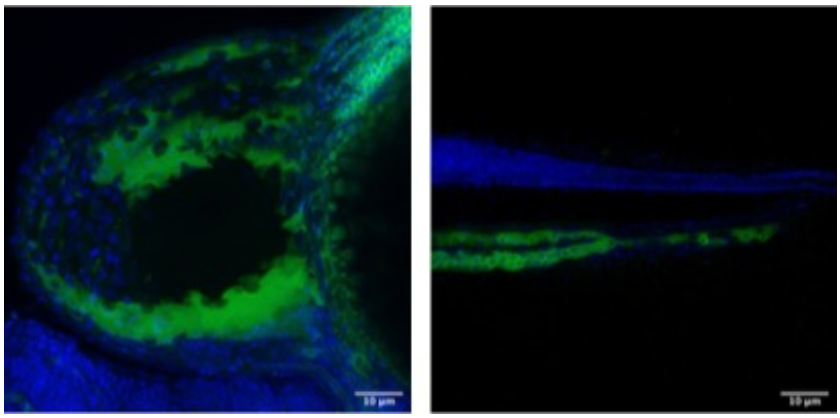

Figure 4.6. Confocal microscope images of 24 hours after the microinjection of Lipofectamine-mRNA complexes (1000 ng mRNA) at the caudal vein of Casper embryos at 48 hpf.

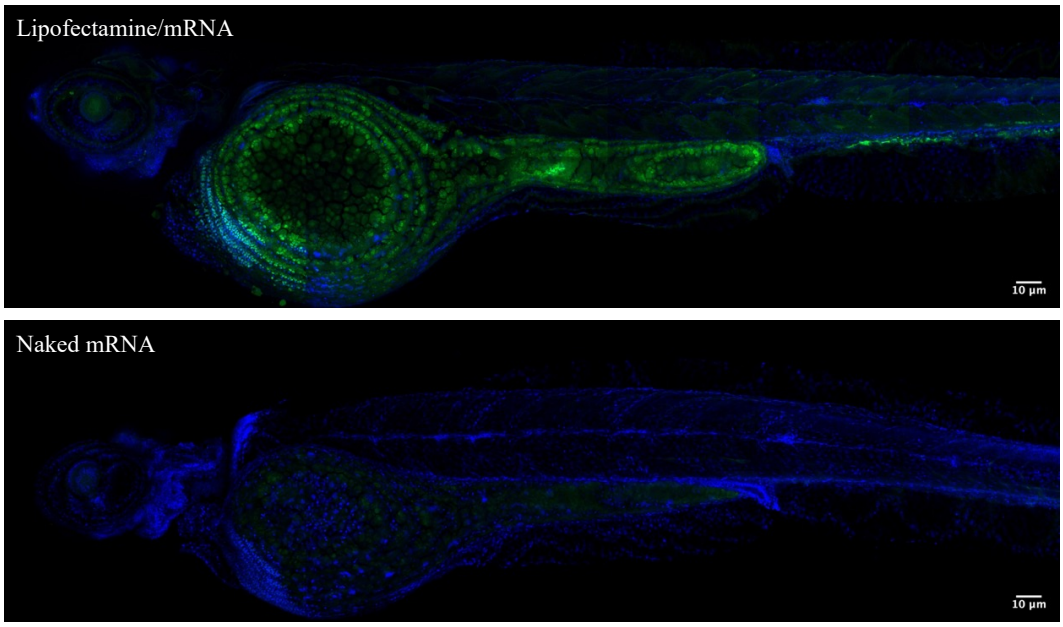

Figure 4.7. Confocal microscope images of Casper type, 48 hpf embryos after microinjection with Lipofectamine-mRNA complexes and naked mRNA (1000 ng) as a control group. The images were taken using 25X objective lens and 24 hours after the microinjection.

Following the investigations performed to observe fluorescence using a stereo microscope (SZX16, Olympus) and after the ideal embryonic stage and injection site had been determined, Lipofectamine-mRNA complexes (containing 1000 ng mRNA) and naked mRNA (1000 ng) were separately microinjected into pericardial cavity of Casper type, 48 hpf embryos for imaging under confocal microscopy. Confocal images were recorded with a 25X objective lens with an interval of 10 μm between each slice (Figure 4.7).

Lastly, a preliminary experiment was performed to verify whether the optimum experimental conditions identified using Lipofectamine-mRNA complexes can be used for transfections with the polymers, PEI (25 kDA) and $P(OEGMA)_{42}$-b-$P(AEAEMA)_{48}$. In this experiment, Casper type embryos (at 48 hpf) were injected at the pericardial cavity with polymer-mRNA (1000 ng) complexes, i.e. $P(OEGMA)_{42}$-b-$P(AEAEMA)_{48}$ polyplexes, at an N/P ratio of 7.3 or 14.4 and the GFP expression was monitored via a stereo microscope after 24 hours. Although GFP irradiation in embryos treated with Lipofectamine-mRNA complexes was observed via a stereo microscope, no irradiation was observed with polyplexes under the same conditions. To obtain GFP reporter expression in zebrafish embryos, the cationic block copolymer complexes containing an increased amount of mRNA (2000 ng) at an N/P ratio of 3.6 or 7.3 were injected into the pericardial cavity of embryos at 48 hpf and the transfection was visualized after 24 hours via microscopy. While no green fluorescence was observed via stereo microscope, the confocal microscope analysis revealed the success of the mRNA transfection. The representative confocal microscope images are shown in Figure 4.8. The images were taken using a 25X lens with a z-stack function of the confocal microscope. As seen in Figure 4.8, in the images taken using DAPI and FITC channels in the injection sites, it was seen that the stained cell nuclei overlapped with the fluorescent regions, especially in the pericardial cavity region. Accordingly, the results obtained with confocal microscopy showed that the mRNA was transfected into the cell, although it was not seen in stereo microscopy.

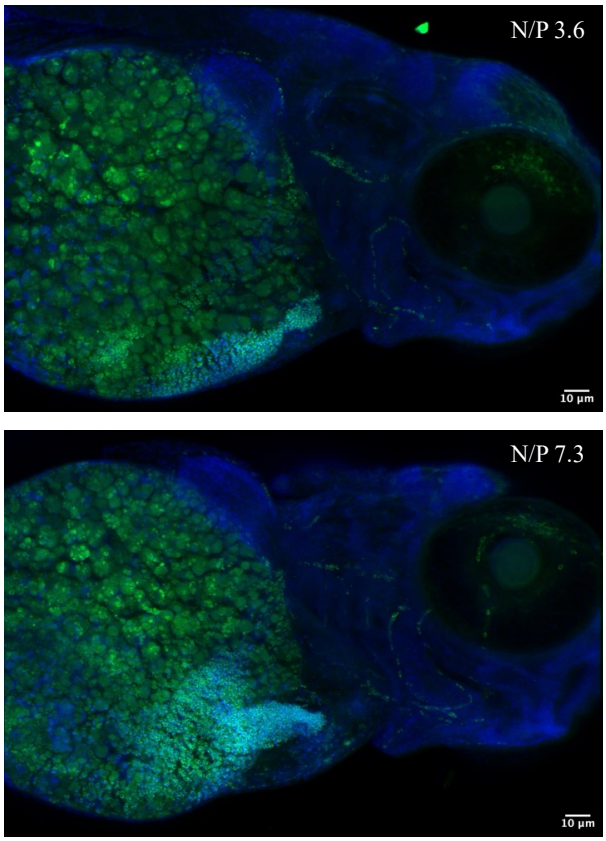

Figure 4.8. Confocal microscope images of Casper embryos at 48 hpf, 24 h after microinjection at the pericardial cavity with P(OEGMA)$_{42}$-b-P(AEAEMA)$_{48}$ - mRNA polyplexes (containing 2000 ng mRNA) (25X lens): N/P 3.6 (above) and N/P 7.3 (below).

Hence, as a result of all the optimization experiments, it was determined that microinjection of polyplex formulation containing 2000 ng mRNA into the pericardial cavity region of Casper type embryos at 48 hpf embryonic stage could be selected for further investigations on the transfection efficiency of polyplexes in this study.

4.2. Formation and Characterization of Polymer-mRNA Polyplexes

Polyplexes with varying N/P ratios containing 1000 ng or 2000 ng of mRNA were initially formed using branched PEI (Mn 25 kDa), which was used as a polymeric control group for transfection experiments. Calculations based on the ratio of the phosphate (P)

groups of the negatively charged mRNA and the cationic amino (N) groups of the polymer were conducted to observe the effect of the varying amounts of polymer while keeping the mRNA amount constant. Polyplexes were formed with different amounts of PEI (0.010 mg, 0.021 mg, and 0.041 mg) using a total of 1000 ng mRNA yielding N/P ratio of 50, 100 and 200, respectively or 2000 ng of mRNA yielding N/P ratio of 25, 50 and 100, respectively. To form complexes with PEI, the required amount of PEI was dissolved in PBS (pH 6.5) to yield the desired polymer concentration. Subsequently, a fixed amount of mRNA (1000 ng or 2000 ng) from the mRNA stock solution was added to the polymer solution. The final volume was kept the same for all polyelectrolyte complex solutions having different polymer concentrations. The final mixtures were kept at room temperature for 25 minutes.

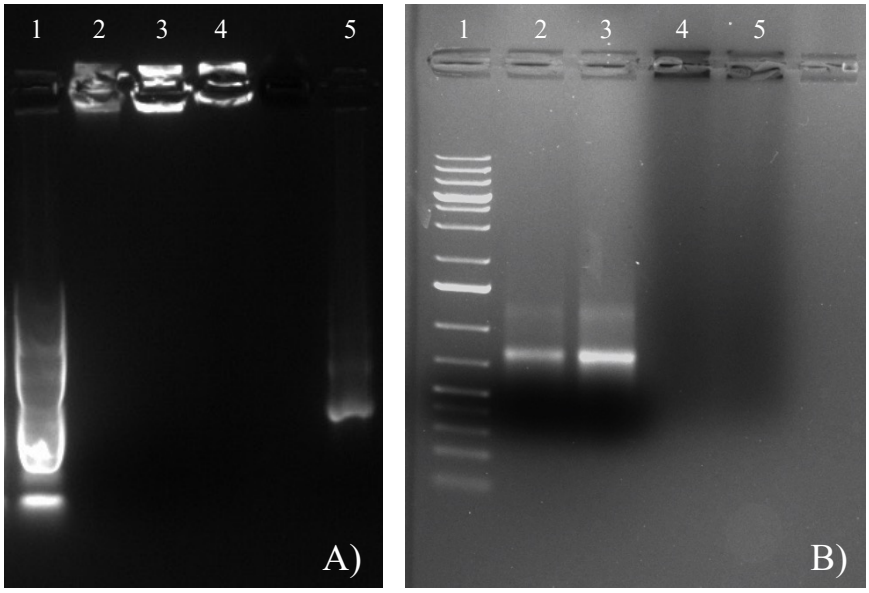

Figure 4.9. (A) Agarose gel electrophoresis result of $P(OEGMA)_{42}$-b-$P(AEAEMA)_{48}$ block copolymer and mRNA polyplexes prepared at varying N/P ratios; Line 1: Marker, Line 2: N/P 3.6, Line 3: N/P 7.3 and Line 4: N/P 10.9 and Line 5: naked GFP mRNA; 7 (B) Agarose gel electrophoresis result of PEI and mRNA polyplexes prepared at varying N/P ratios; Line 1: Marker, Line 2: 1000 ng naked GFP mRNA, Line 3: 2000 ng naked GFP mRNA and Line 4: N/P 50 (2000 ng GFP mRNA) and Line 5: N/P 100 (1000 ng GFP mRNA).

The same protocol for the complexation experiment was performed for $P(OEGMA)_{42}$-b-$P(AEAEMA)_{48}$ cationic block copolymer. The polyplexes were formed at N/P 3.6, N/P 7.3 and N/P 10.9 ratios with 0.015 mg, 0.030 mg, and 0.045 mg block copolymer amounts respectively. The agarose gel electrophoresis was used to determine the N/P ratio at which the whole amount of mRNA was complexed with the polymers. It was expected that the polymers forming complexes with the mRNA would restrict the movement of negatively charged mRNA under the electric field, resulting in no visible bands. The results are presented in Figure 4.9A and B. As seen in the figure, the naked mRNA and marker line were visible under UV light, while no bands were observed in the polyplex structures due to the polymers binding with the mRNA. This indicated that the polyplexes of $P(OEGMA)_{42}$-b-$P(AEAEMA)_{48}$ and mRNA (2000 ng) were successfully formed even at an N/P ratio of 3.6. PEI was able to complex with 1000 ng mRNA at an N/P ratio of 100 and 2000 ng mRNA at an N/P ratio of 50.

4.3. mRNA Transfection Efficiency of Polyplexes

Naked embryo, naked mRNA, Lipofectamine-mRNA complex, PEI-mRNA and $P(OEGMA)_{42}$-b-$P(AEAEMA)_{48}$–mRNA polyplexes were used for evaluation of transfection. Firstly, 48 hpf zebrafish embryos were physically removed from their chorions and anesthetized with Tricaine (10 mg/ml). Transfection experiments were performed by microinjection of samples into the pericardial cavity of 48 hpf zebrafish embryos under the same conditions as previously described. Approximately 40 nl of polyplex solution was injected into each embryo. Injected embryos were incubated for 24 hours at 28^{o}C in E3 zebrafish embryo medium (NaCl, KCl, $CaCl_2 \cdot 2H_2O$, and $MgCl_2 \cdot 6H_2O$ and pH 7.2). The embryos were monitored using stereo microscopy at specified time intervals, and teratogenic malformations were examined under the microscope. Teratogenesis and mortality were high for PEI-mRNA complexes with an N/P ratio greater than 100 and a total mRNA of 1000 ng, exhibiting toxic effects in embryos and the survival rate was less than 80%. On the other hand, it was observed that PEI complexes with mRNA (2000 ng) at an N/P ratio of 50 showed tolerable toxicity (>80%).

P(OEGMA)$_{42}$-b-P(AEAEMA)$_{48}$-mRNA complexes having an mRNA dose of 2000 ng and an N/P ratio of 14.4 and above resulted in survival rates below 80%. Therefore, lower N/P ratios (3.6 or 7.3) were preferred for transfection experiments of P(OEGMA)$_{42}$-b-P(AEAEMA)$_{48}$-mRNA complexes. Transfection efficiencies were evaluated only using an N/P ratio of 50 for PEI, and N/P ratios of 3.6 and 7.3 for the block copolymer, P(OEGMA)$_{42}$-b-P(AEAEMA)$_{48}$ using GFP mRNA (2000 ng). Naked mRNA (2000 ng) was used as a negative control group and Lipofectamine-mRNA complexes (containing 2000 ng mRNA) were used as a positive control for transfection experiments. Embryos were injected with the respective sample solution, incubated for 24 hours at 28^{o}C in E3 zebrafish embryo medium (NaCl, KCl, $CaCl_2 \cdot 2H_2O$, and $MgCl_2 \cdot 6H_2O$ and pH 7.2), and then embryos were fixed. Immunostaining and mounting procedures were performed for imaging under confocal microscopy which allowed to visualize mRNA transport thanks to the transparency of zebrafish embryos. Images were analyzed via a 25X and 63X objective lens using DAPI (blue) and FITC (green) channels.

Confocal microscopy analysis of two randomly selected samples treated with Lipofectamine-mRNA complexes revealed significant GFP expression (Figure 4.10) distributed beyond the injected site. Furthermore, the confocal microscopy images of two randomly selected samples treated with PEI-mRNA (2000 ng) complexes at N/P=50 is shown in Figure 4.11.

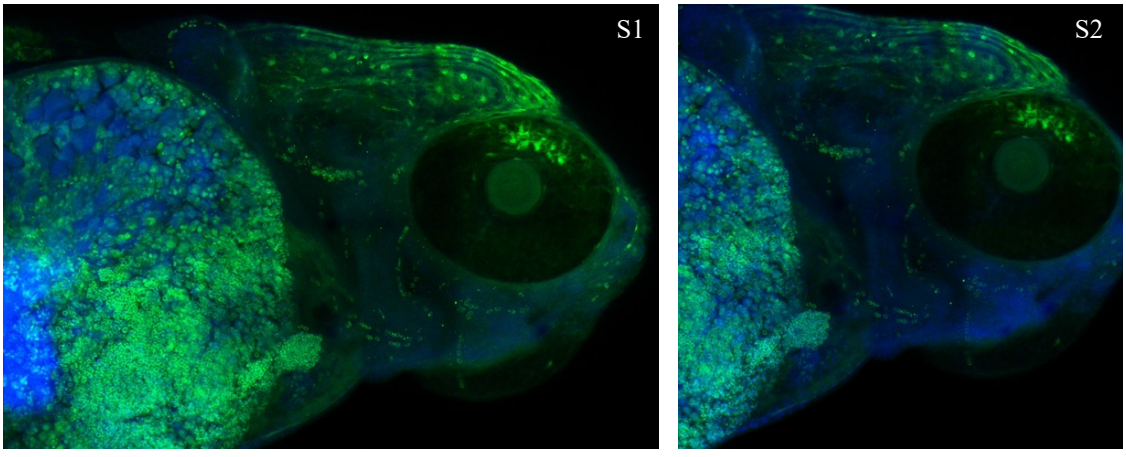

Figure 4.10. Confocal microscope images of two different Casper embryos at 48 hpf 24 hours after the microinjection with Lipofectamine- mRNA complexes (2000 ng mRNA) at the pericardial cavity: Sample 1 (S1) and Sample 2 (S2). (25X lens).

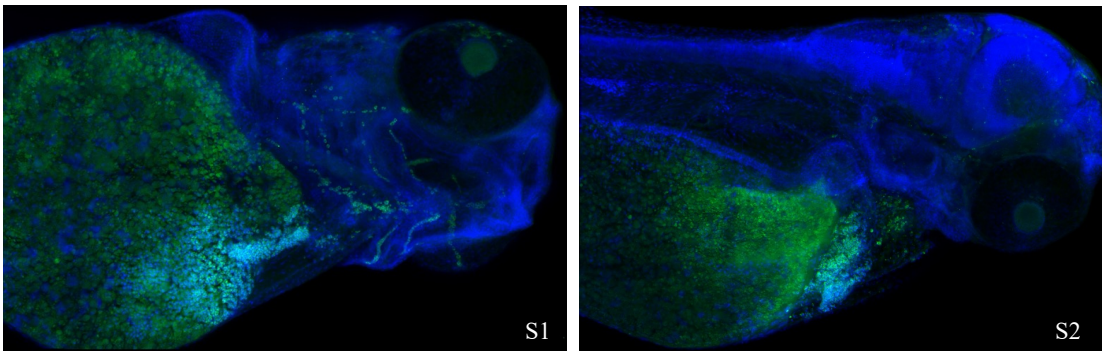

Figure 4.11. Confocal microscope images of two different Casper embryos at 48 hpf 24 hours after the microinjection with PEI-mRNA complexes (2000 ng mRNA) at N/P=50 at the pericardial cavity: Sample 1 (S1) and Sample 2 (S2). (25X lens).

Confocal microscopy images of three different zebrafish embryo samples treated with P(OEGMA)$_{42}$-b-P(AEAEMA)$_{48}$-mRNA complexes (at an N/P=3.6 and 7.3) are shown in Figure 4.12. The GFP expressions were found to localize around the injected region and showed comparable fluorescence with Lipofectamine complexes. Of the two different N/P ratios, with an N/P of 7.3 more GFP expression was observed.

In addition to the images taken using a 25X lens, the same specimens were examined more closely using a 63X lens on a confocal microscope in order to focus only on the injected area, the pericardial cavity, and to provide quantitative data. These results were analyzed by randomly selecting 3 samples (N=3). Figure 4.13 to Figure 4.16 were presented as representation data. All repeated results for each group are shown in Appendix A (Figure A1 to Figure A6). Naked embryos used as a control group were analyzed to establish a baseline. Injections of naked GFP mRNA showed very little GFP expression (Figure 4.13). The complex formed with Lipofectamine, a commercial agent commonly used in cell experiments, showed better results compared to the naked embryo (Figure 4.14). Polyplexes formed with PEI (MW=25 kDA) showed much higher transfection efficiency than the other groups. The number of cells stained with DAPI was quite high for the embryos treated with the polyplexes of PEI. In addition, there was an overlap with the FITC images shown in green (Figure 4.15). Colocalized blue and green regions confirmed that the injected mRNA was efficiently taken up by the cells and translated into GFP expression. As seen in Figure 4.16, the confocal microscope images also revealed significantly high mRNA transfection with P(OEGMA)$_{42}$-b-P(AEAEMA)$_{48}$

block copolymer with respect to the negative control group. Cells with N/P 3.6 ratio showed higher transfection efficiency compared to N/P 7.3 ratio. Compared to PEI-mRNA complexes, transfection of cells using block copolymer complexes with N/P 7.3 ratio showed lower efficiency.

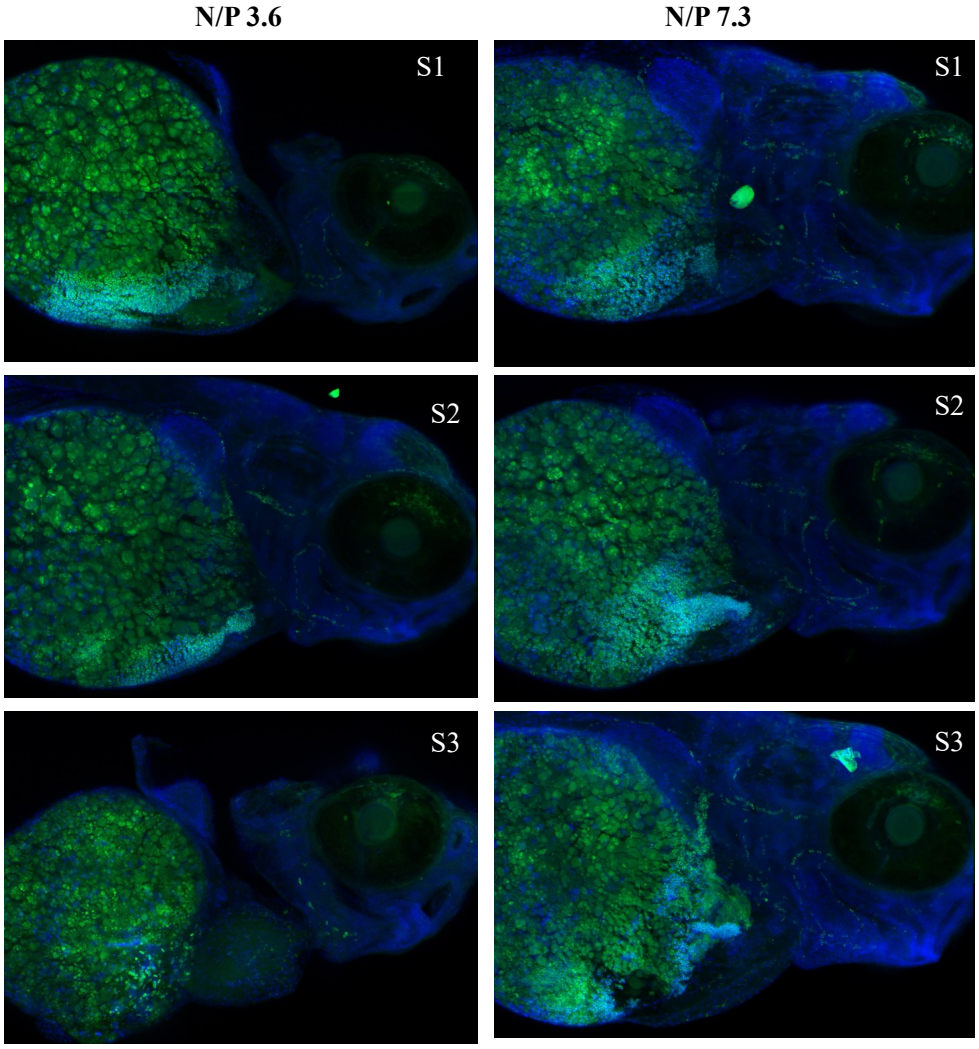

Figure 4.12. Confocal microscope images of three different Casper embryos (S1, S2, S3) at 48 hpf 24 hours after the microinjection with P(OEGMA)$_{42}$-b-P(AEAEMA)$_{48}$ -mRNA polyplexes (containing 2000 ng mRNA) at the pericardial cavity: N/P= 3.6 (left) and N/P= 7.3 (right). (25X lens).

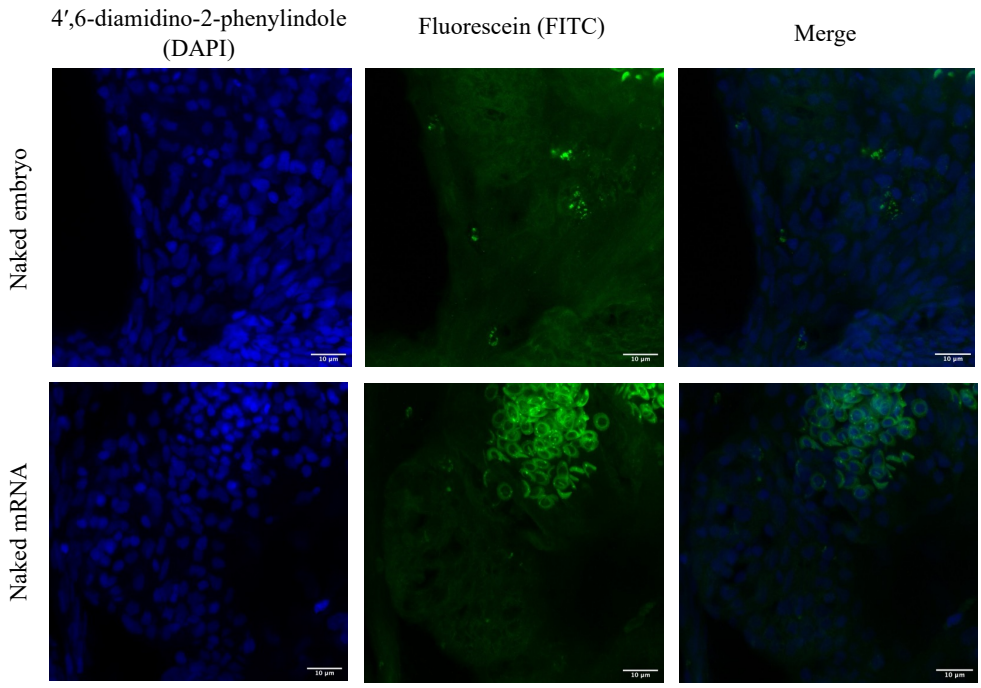

Figure 4.13. Confocal microscope results of transfection experiments: Control groups only.

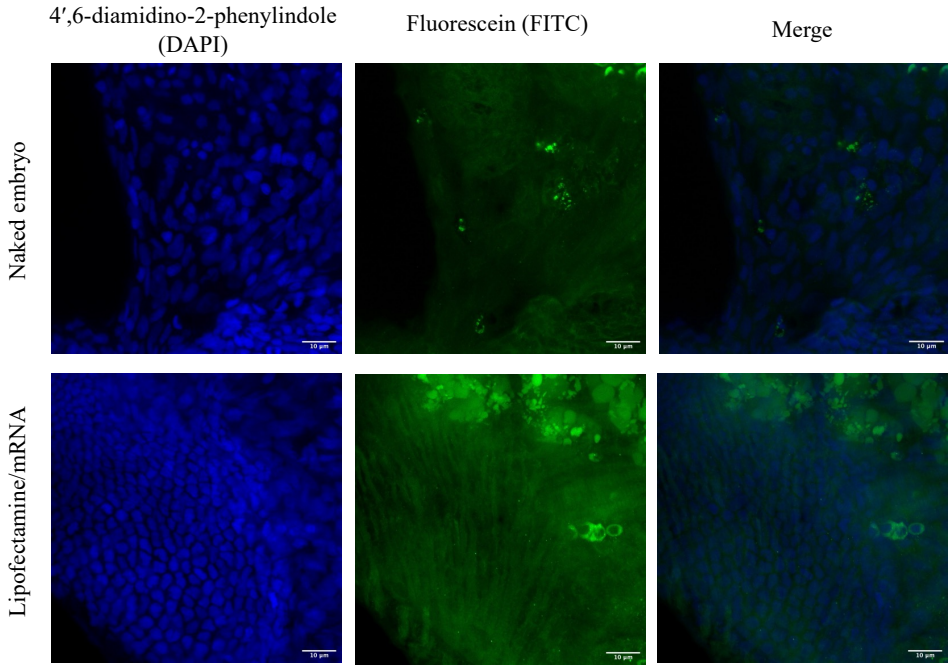

Figure 4.14. Confocal microscope results of transfection experiments: Lipofectamine-mRNA complexes.

All experiments confirmed the colocalization (in cyan) of DAPI and FITC in embryo samples treated with the block copolymer-mRNA polyplexes. This overlapping proves that mRNA transfection efficiently resulted in the expression of GFP protein by the cells. This key step clearly showed the ability of $P(OEGMA)_{42}$-b-$P(AEAEMA)_{48}$ block copolymer to transport the cargo mRNA into the cells. Moreover, the different proportions of the cytoplasmic region around the cell nuclei confirmed that the transfection efficiently occurred in the cytoplasmic phase.

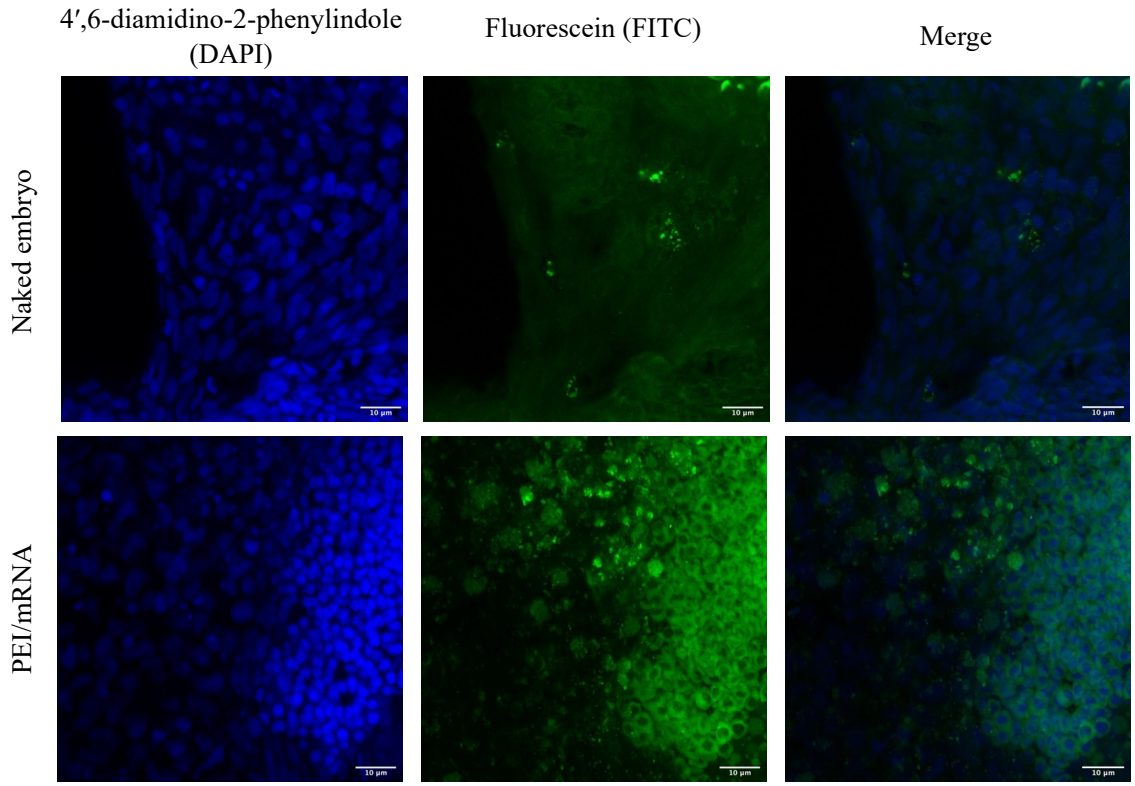

Figure 4.15. Confocal microscope results of transfection experiments: PEI-mRNA polyplexes with an N/P ratio of 50 (2000 ng GFP mRNA).

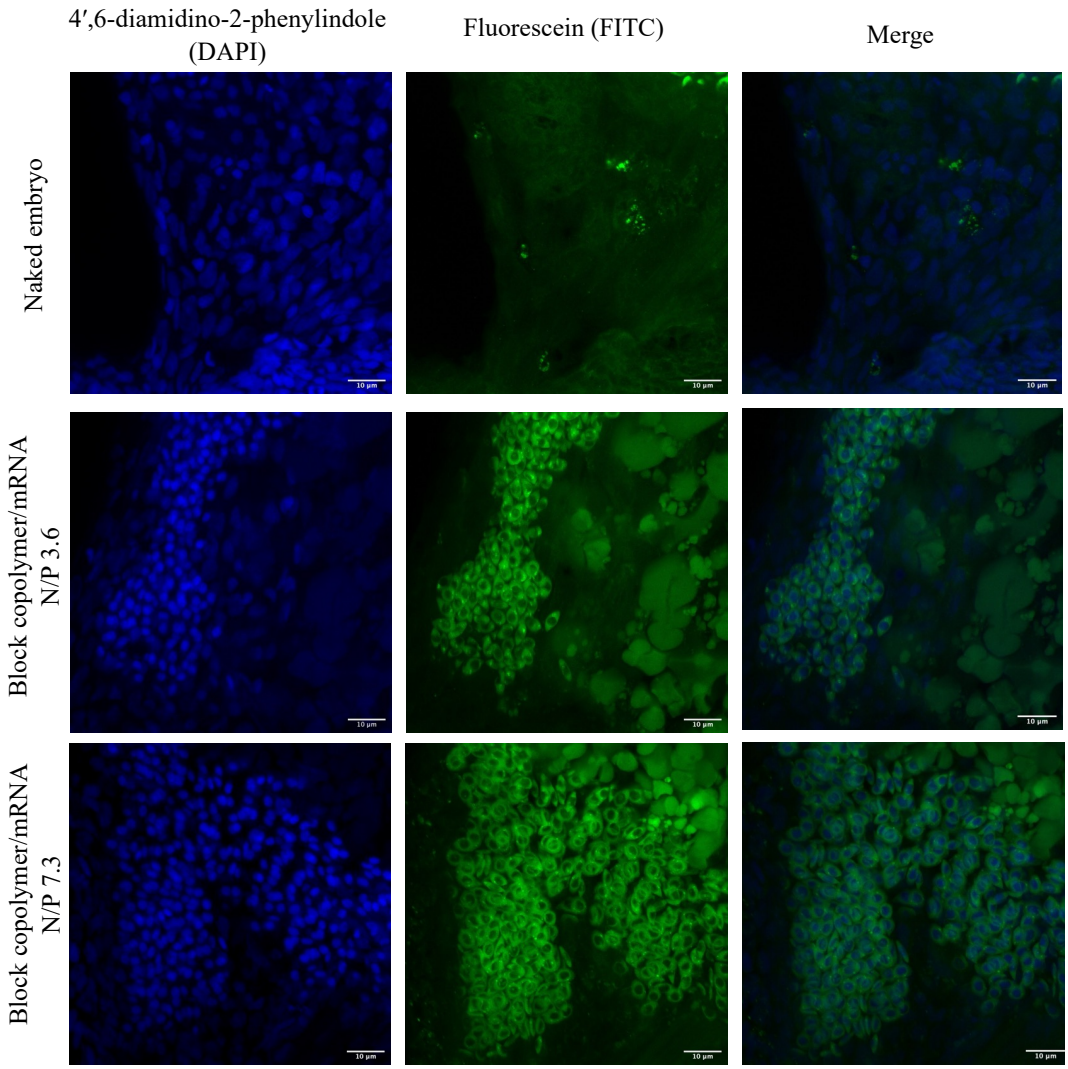

Figure 4.16. Confocal microscope results of transfection experiments: $P(OEGMA)_{42}$-b-$P(AEAEMA)_{48}$ -mRNA polyplexes with an N/P ratio of 3.6 and 7.3.

The ImageJ program was used for data analysis of the results obtained from confocal images. The cells delimited using the threshold level feature were then made black and white with the make binary function. The watershed function was used to separate adjacent cells and make the analysis more accurate. The representative data obtained after these operations are presented in Figure 4.17. Results of all replicate experiments for each group are also shown in Appendix B (Figure B1 and Figure B2). Finally, the number of cells was calculated using the analyze particle function under the analysis tab. The whole image size (20 μm) was used for the cell number analysis of different samples. Accordingly, the highest transfection efficiency was found with mRNA

complexed with PEI at an N/P ratio of 50. The results were quite close for Lipofectamine-mRNA and block copolymer-mRNA complexes of an N/P ratio of 3.6. A slightly lower transfection efficiency was obtained in the experiments performed with the block copolymer at an N/P ratio of 7.3. Some studies have shown that although Lipofectamine can be used effectively in *in vitro* studies, other gene delivery methods are more efficient and safer for *in vivo* use. Lipofectamine has several limitations when used *in vivo*, such as toxicity and inconsistent delivery efficiency. These limitations make Lipofecatime less suitable for *in vivo* applications (Sohi et al. 2021). Although GFP expression was observed specifically at the site of injection in samples with polymer-based mRNA, samples injected with Lipofectamine-mRNA complex appeared to completely diffuse throughout the whole body especially in the head region. Therefore, less GFP expression was observed in the pericardial region of Lipofectamine-mRNA injected samples. All data calculated from ImageJ software supported the visually obtained results.

To further verify the results obtained from the overlap regions, the number of cells was calculated from the images obtained separately from the DAPI and FITC channels of the confocal microscope, again using the ImageJ program. The cell number analysis was then plotted as shown in Figure 4.18. Also, the integrated density of the cell fluorescence was measured from the images obtained from the FITC channels of the confocal microscope, again using the ImageJ program. To eliminate the background fluorescence readings, the corrected total cell fluorescence (CTCF) was calculated from the CTCF formula. The CTCF was calculated according to the following;

CTCF = Integrated Density – [Area of selected cell X Mean fluorescence of background readings (naked embryo)] (Measuring Cell Fluorescence Using ImageJ, The Open Lab Book)

All calculated CTCF findings are presented in Figure 4.19. Furthermore, transfection efficiency was calculated as a percentage of the FITC intensity of cells of embryos after different treatments to the FITC intensity of cells of naked embryos (Figure 4.20). The results are presented as mean±standard error (N= 3).

Consequently, the polyplexes obtained using block copolymer at an N/P ratio of 7.3 showed the highest yield according to the intensity measurement. PEI-mRNA and block copolymer-mRNA polyplexes having N/P ratio of 3.6 showed similar results. Lipofectamine, which showed high amounts of observable GFP fluorescence outside the injected region, showed low transfection efficiency in cells of pericardial region.

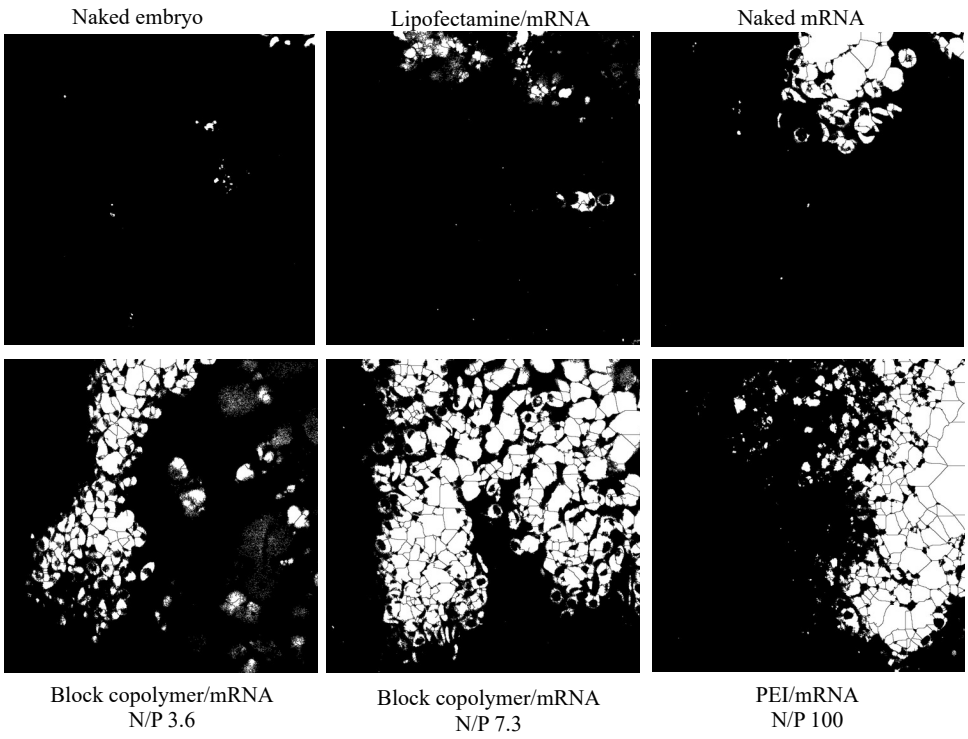

Figure 4.17. Visualization of overlapping cells analyzed using the threshold function in ImageJ.

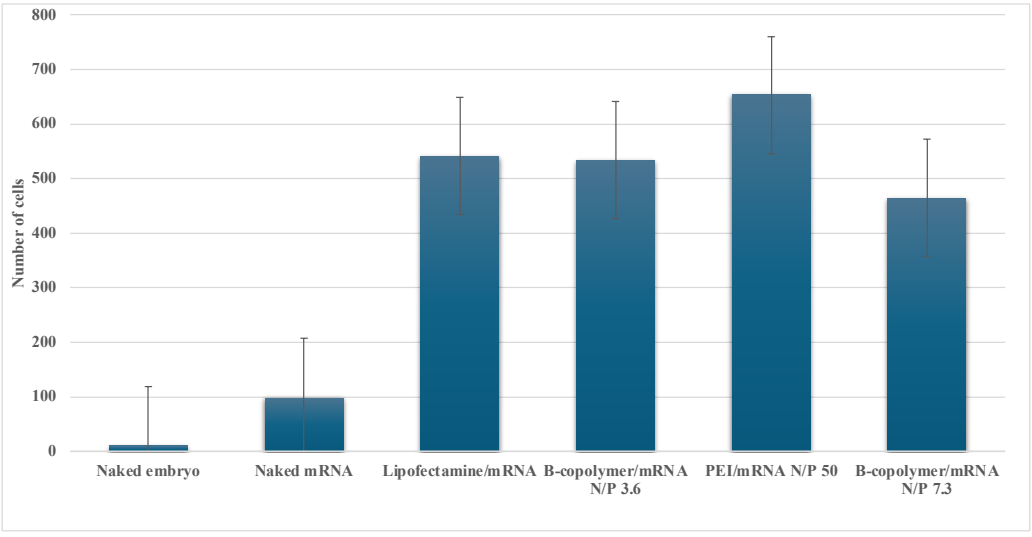

Figure 4.18. Colocalized cell number measurements using ImageJ software. The results are presented as mean±standard error (N= 3).

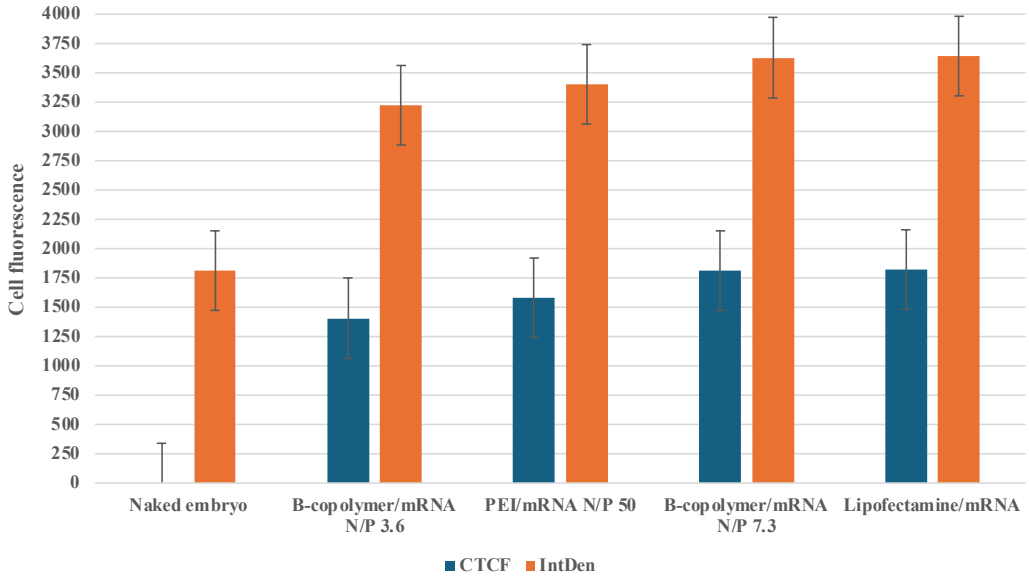

Figure 4.19. Integrated density measurement using ImageJ software measurement function from analyze menu and calculation results of the corrected total cell fluorescence (CTCF). The results are presented as mean±standard error (N= 3).

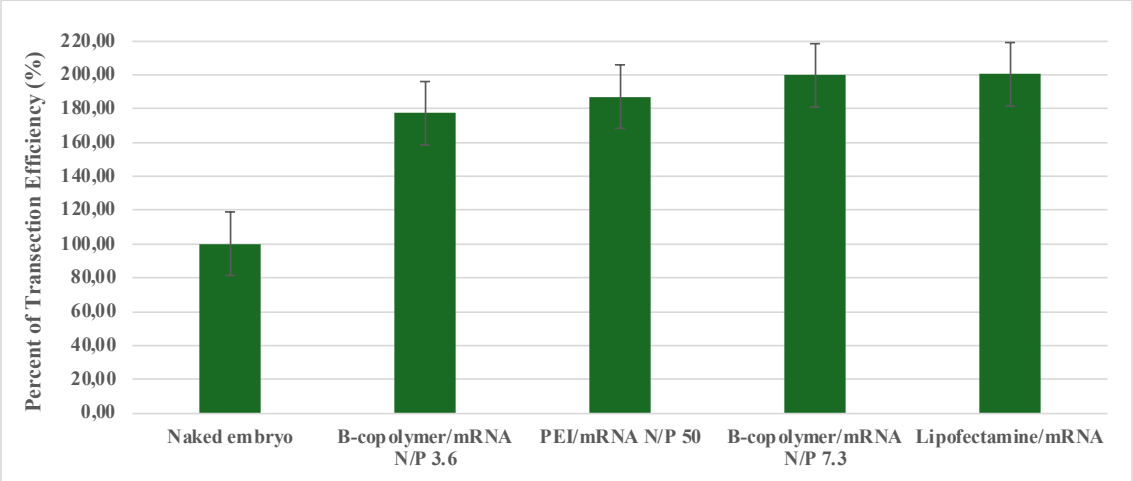

Figure 4.20. Transection efficiency (%) based on the FITC intensity of cells of embryos after different treatments normalized to the FITC intensity of cells of naked embryos using ImageJ software measurement function. The results are presented as mean±standard error (N= 3).

CHAPTER 5

CONCLUSION

Developing safe and efficient vectors capable of delivering therapeutic genes to target cells is still an important need for treatment of numerous diseases including cancer. *In vivo* studies are crucial in the transition of developed vectors to clinical use. This thesis aimed to perform a preliminary investigation on the *in vivo* transfection potential of $P(OEGMA)_{42}$-b-$P(AEAEMA)_{48}$ block copolymer, for which *in vitro* studies were previously completed (Savas 2023, 25-46), as an mRNA carrier agent. For this purpose, the zebrafish embryo model was used as a bridge to experimental animals such as mice. The optimal conditions for *in vivo* transfection experiments using the zebrafish model were first determined. Various parameters including zebrafish type (Casper type and/or AB type), embryonic developmental stage (0 hpf, 24 hpf, 48 hpf), injection site (pericardial cavity, trunk, circulation), mRNA administration method were separately investigated. Considering the results obtained from optimization analysis, polyplexes formed with eGFP-mRNA (2000 ng) and $P(OEGMA)_{42}$-b-$P(AEAEMA)_{48}$ at an N/P ratio of 3.6 or 7.3 were injected into the pericardial cavity of developing zebrafish embryos at 48 hours post fertilization (hpf) to observe GFP expression. Naked mRNA, naked embryos, Lipofectamine-mRNA complex, and PEI-mRNA polyplexes were used for comparison. Samples were visualized 24 hours after injection using confocal microscopy and analyzed with Image J software. The block copolymer showed transfection efficiency comparable with the golden standard polymeric vector PEI. Compared to the naked embryo, polyplexes formed with cationic polymers showed high transfection efficiency. According to analysis from the colocalized blue and green regions, PEI-mRNA complexes treated samples were shown the highest cell number. When transfection efficiency was measured from the FITC intensity, samples treated with cationic polymer-mRNA showed a high ratio.

In summary, this thesis demonstrated the potential of a new polymeric system for mRNA delivery and reported preliminary results based on *in vivo* investigations using

zebrafish embryos. It further established experimental parameters for well-known transfection agents, Lipofectamine 3000 and b-PEI (25 kDa). Some suggestions to improve the current study are as follows:

i. Transfection experiments need to be repeated further to take confocal microscope images from different regions of the zebrafish embryo to analyze the transfection efficiency more accurately.

ii. Embryos can be observed for longer hours after injection to examine the effect of time on GFP expression.

iii. For PEI, optimization of transfection experiments can be done using lower N/P ratios.

iv. Transfection experiments can also be performed in adult zebrafish embryos.

REFERENCES

Bondue, Tjessa, Sante Princiero Berlingerio, Lambertus Van Den Heuvel, and Elena Levtchenko. 2023. "The Zebrafish Embryo as a Model Organism for Testing mRNA-Based Therapeutics." International Journal of Molecular Sciences 24, no. 13 (July): 11224. https://doi.org/10.3390/ijms241311224.

Cascallar, María, Pablo Hurtado, Saínza Lores, Alba Pensado-López, Ana Quelle-Regaldie, Laura Sánchez, Roberto Piñeiro, and María De La Fuente. 2022. "Zebrafish as a Platform to Evaluate the Potential of Lipidic Nanoemulsions for Gene Therapy in Cancer." Frontiers in Pharmacology 13 (October). https://doi.org/10.3389/fphar.2022.1007018.

Chen, Jiaxuan, Dandan Zhu, Xiaoxuan Liu, and Ling Peng. 2022. "Amphiphilic Dendrimer Vectors for RNA Delivery: State-of-the-Art and Future Perspective." Accounts of Materials Research 3, no. 5 (May): 484–97. https://doi.org/10.1021/accountsmr.1c00272.

Dakwar, George R., Kevin Braeckmans, Joseph Demeester, Wim Ceelen, Stefaan C. De Smedt, and Katrien Remaut. 2015. "Disregarded Effect of Biological Fluids in siRNA Delivery: Human Ascites Fluid Severely Restricts Cellular Uptake of Nanoparticles." ACS Applied Materials & Interfaces 7, no. 43 (October): 24322–29. https://doi.org/10.1021/acsami.5b08805.

Debus, Heiko, Patrick Baumhof, Jochen Probst, and Thomas Kissel. 2010. "Delivery of Messenger RNA Using Poly(Ethylene Imine)–poly(Ethylene Glycol)-copolymer Blends for Polyplex Formation: Biophysical Characterization and *in Vitro* Transfection Properties." Journal of Controlled Release 148, no. 3 (December): 334–43. https://doi.org/10.1016/j.jconrel.2010.09.007.

Fenaroli, Federico, David Westmoreland, Jørgen Benjaminsen, Terje Kolstad, Frode Miltzow Skjeldal, Annemarie H. Meijer, Michiel Van Der Vaart, et al. 2014. "Nanoparticles as Drug Delivery System Against Tuberculosis in Zebrafish Embryos: Direct Visualization and Treatment." ACS Nano 8, no. 7 (June): 7014–26. https://doi.org/10.1021/nn5019126.

Goudy, Julie, Trevor Henley, Hernán G. Méndez, and Michael Bressan. 2019. "Simplified Platform for Mosaic *in Vivo* Analysis of Cellular Maturation in the Developing Heart." Scientific Reports 9, no. 1 (July). https://doi.org/10.1038/s41598-019-47009-7.

Hu, Qinglian, Fengliang Guo, Fenghui Zhao, Guping Tang, and Zhengwei Fu. 2017. "Cardiovascular Toxicity Assessment of Poly (Ethylene Imine)- Based Cationic Polymers on Zebrafish Model." *Journal of Biomaterials Science, Polymer Edition* 28 (8): 768–80. doi:10.1080/09205063.2017.1301773.

Islam, Mohammad Ariful, Emma K. G. Reesor, Yingjie Xu, Harshal R. Zope, Bruce R. Zetter, and Jinjun Shi. 2015. "Biomaterials for mRNA Delivery." Biomaterials Science 3, no. 12 (January): 1519–33. https://doi.org/10.1039/c5bm00198f.

Kamegawa, Rimpei, Mitsuru Naito, Satoshi Uchida, Hyun Jin Kim, Beob Soo Kim, and Kanjiro Miyata. 2021. "Bioinspired Silicification of mRNA-Loaded Polyion Complexes for Macrophage-Targeted mRNA Delivery." ACS Applied Bio Materials 4, no. 11 (October): 7790–99. https://doi.org/10.1021/acsabm.1c00704.

Kim, Jeonghwan, Yulia Eygeris, Mohit Gupta, and Gaurav Sahay. 2021. "Self-assembled mRNA Vaccines." Advanced Drug Delivery Reviews 170 (March): 83–112. https://doi.org/10.1016/j.addr.2020.12.014.

''Lipofectamine™ 3000 Reagent Protocol.'' February 10, 2016. https://assets.thermofisher.com/TFSAssets/LSG/manuals/lipofectamine3000_protocol.pdf.

Liu, Ming-Xuan, Le-Le Ma, Xu-Ying Liu, Jin-Yu Liu, Zhong-Lin Lu, Rui Liu, and Lan He. 2019. "Combination of [12]aneN3 and Triphenylamine-Benzylideneimidazolone as Nonviral Gene Vectors With Two-Photon and AIE Properties." ACS Applied Materials & Interfaces 11, no. 46 (October): 42975–87. https://doi.org/10.1021/acsami.9b15169.

Martinez-Lopez, Mayra, Vanda Póvoa, and Rita Fior. 2021. "Generation of Zebrafish Larval Xenografts and Tumor Behavior Analysis." *Journal of Visualized Experiments*, no. 172 (June). https://doi.org/10.3791/62373.

''Measuring Cell Fluorescence Using ImageJ — the Open Lab Book v1.0'' n.d. https://theolb.readthedocs.io/en/latest/imaging/measuring-cell-fluorescence-using-imagej.html.

Mohammadi-Samani, Soliman, and Parisa Ghasemiyeh. 2018. "Solid Lipid Nanoparticles and Nanostructured Lipid Carriers as Novel Drug Delivery Systems: Applications, Advantages and Disadvantages." Research in Pharmaceutical Sciences 13, no. 4 (January): 288. https://doi.org/10.4103/1735-5362.235156.

Molla, Mijanur R., Shraddha Chakraborty, Leonel Munoz−Sagredo, Markus Drechsler, Véronique Orian−Rousseau, and Pavel A. Levkin. 2020. "Combinatorial Synthesis of a Lipidoid Library by Thiolactone Chemistry: *In Vitro* Screening and *in Vivo* Validation for siRNA Delivery." Bioconjugate Chemistry 31, no. 3 (February): 852–60. https://doi.org/10.1021/acs.bioconjchem.0c00013.

Najer, Adrian, Joshua Blight, Catherine B. Ducker, Matteo Gasbarri, Jonathan C. Brown, Junyi Che, Håkon Høgset, et al. 2022. "Potent Virustatic Polymer–Lipid Nanomimics Block Viral Entry and Inhibit Malaria Parasites *in Vivo*." ACS Central Science 8, no. 9 (May): 1238–57. https://doi.org/10.1021/acscentsci.1c01368.

Olden, Brynn R., Yilong Cheng, Jonathan L. Yu, and Suzie H. Pun. 2018. "Cationic Polymers for Non-viral Gene Delivery to Human T Cells." Journal of Controlled Release 282 (July): 140–47. https://doi.org/10.1016/j.jconrel.2018.02.043.

Pack, Daniel W., Allan S. Hoffman, Suzie Pun, and Patrick S. Stayton. 2005. "Design and Development of Polymers for Gene Delivery." Nature Reviews. Drug Discover/Nature Reviews. Drug Discovery 4, no. 7 (July): 581–93. https://doi.org/10.1038/nrd1775.

Paunovska, Kalina, David Loughrey, and James E. Dahlman. 2022. "Drug Delivery Systems for RNA Therapeutics." Nature Reviews. Genetics 23, no. 5 (January): 265–80. https://doi.org/10.1038/s41576-021-00439-4.

''Polyethylenimine, Branched," Merck, n.d., https://www.sigmaaldrich.com/TR/en/product/aldrich/408727.

Rizzo, Larissa Y., Susanne K. Golombek, Marianne E. Mertens, Yu Pan, Dominic Laaf, Janine Broda, Jabadurai Jayapaul, et al. 2013. "In Vivo Nanotoxicity Testing Using the Zebrafish Embryo Assay." *Journal of Materials Chemistry B* 1 (32): 3918. https://doi.org/10.1039/c3tb20528b.

Sago, Cory D., Melissa P. Lokugamage, Kalina Paunovska, Daryll A. Vanover, Christopher M. Monaco, Nirav N. Shah, Marielena Gamboa Castro, et al. 2018. "High-throughput *in Vivo* Screen of Functional mRNA Delivery Identifies Nanoparticles for Endothelial Cell Gene Editing." Proceedings of the National Academy of Sciences of the United States of America 115, no. 42 (October). https://doi.org/10.1073/pnas.1811276115.

Sant, K. E., Timme-Laragy, A. R. 2018. ‘’*Zebrafish as a Model for Toxicological Perturbation of Yolk and Nutrition in the Early Embryo. Current environmental health reports.’’*5(1), 125–133. https://doi.org/10.1007/s40572-018-0183-2

Savas, Müge. 2023. “Development of Polymeric Carriers for Mrna Delivery.” Master Thesis, Izmir Institute of Technology.

Sohi, Alireza Naderi, Jafar Kiani, Ehsan Arefian, Arezou Khosrojerdi, Zahra Fekrirad, Shokoofeh Ghaemi, Mohammad Kazem Zim, Arsalan Jalili, Nazila Bostanshirin, and Masoud Soleimani. 2021. “Development of an mRNA-LNP Vaccine Against SARS-CoV-2: Evaluation of Immune Response in Mouse and Rhesus Macaque.” Vaccines 9, no. 9 (September): 1007. https://doi.org/10.3390/vaccines9091007.

Wang, Fang, Lu Gao, Liu-Yi Meng, Jing-Ming Xie, Jing-Wei Xiong, and Ying Luo. 2016. “A Neutralized Noncharged Polyethylenimine-Based System for Efficient Delivery of Sirna into Heart without Toxicity.” ACS Applied Materials & Interfaces 8, no. 49 (December): 33529–38. https://doi.org/10.1021/acsami.6b13295.

Witzigmann, Dominik, Dalin Wu, Susanne H. Schenk, Vimalkumar Balasubramanian, Wolfgang Meier, and Jörg Huwyler. 2015. “Biocompatible Polymer–Peptide Hybrid-Based DNA Nanoparticles for Gene Delivery.” ACS Applied Materials & Interfaces 7, no. 19 (May): 10446–56. https://doi.org/10.1021/acsami.5b01684.

Yan, Yunfeng, Hu Xiong, Xinyi Zhang, Qiang Cheng, and Daniel J. Siegwart. 2017. “Systemic mRNA Delivery to the Lungs by Functional Polyester-based Carriers.” Biomacromolecules 18, no. 12 (November): 4307–15. https://doi.org/10.1021/acs.biomac.7b01356.

Zelçak, Aykut. 2021. “Development of Novel Polymer|c Carr|ers for Gene Therapy.” Doctoral Thesis, Izmir Institute of Technology.

Zhang, Yuebao, Changzhen Sun, Chang Wang, Katarina E. Jankovic, and Yizhou Dong. 2021. “Lipids and Lipid Derivatives for RNA Delivery.” Chemical Reviews 121, no. 20 (July): 12181–277. https://doi.org/10.1021/acs.chemrev.1c00244.

Zhang, Yuyan, Yingying Hu, Huayu Tian, and Xuesi Chen. 2022. “Opportunities and Challenges for mRNA Delivery Nanoplatforms.” The Journal of Physical Chemistry Letters 13, no. 5 (February): 1314–22. https://doi.org/10.1021/acs.jpclett.1c03898.

APPENDIX A

CONFOCAL MICROSCOPE RESULTS OF TRANSFECTION EXPERIMENTS

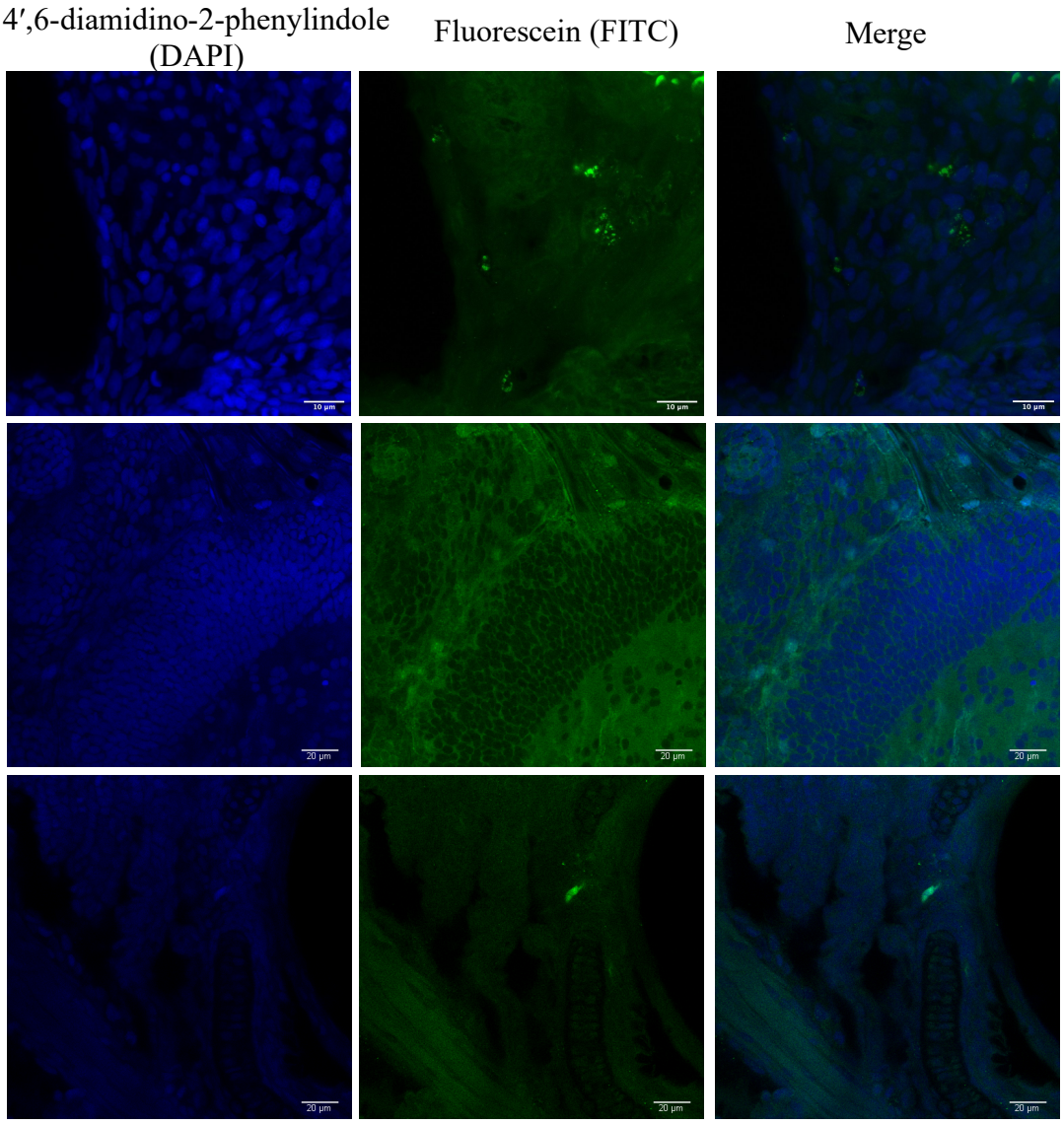

Figure A1. Confocal microscope results of three different naked embryo samples randomly selected from transfection experiments performed as a negative control.

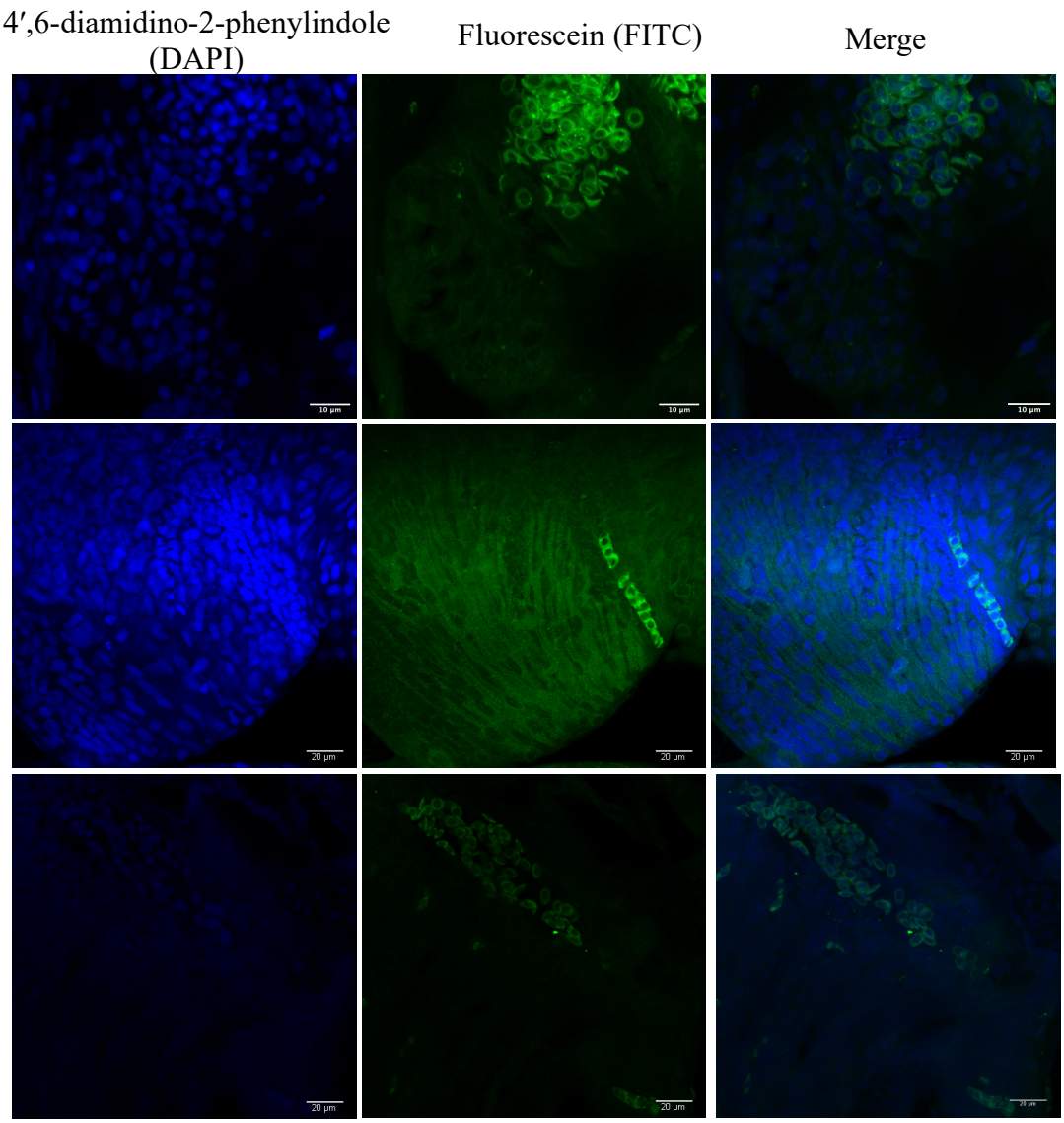

Figure A2. Confocal microscope results of three different samples randomly selected from transfection experiments performed using naked mRNA (2000 ng).

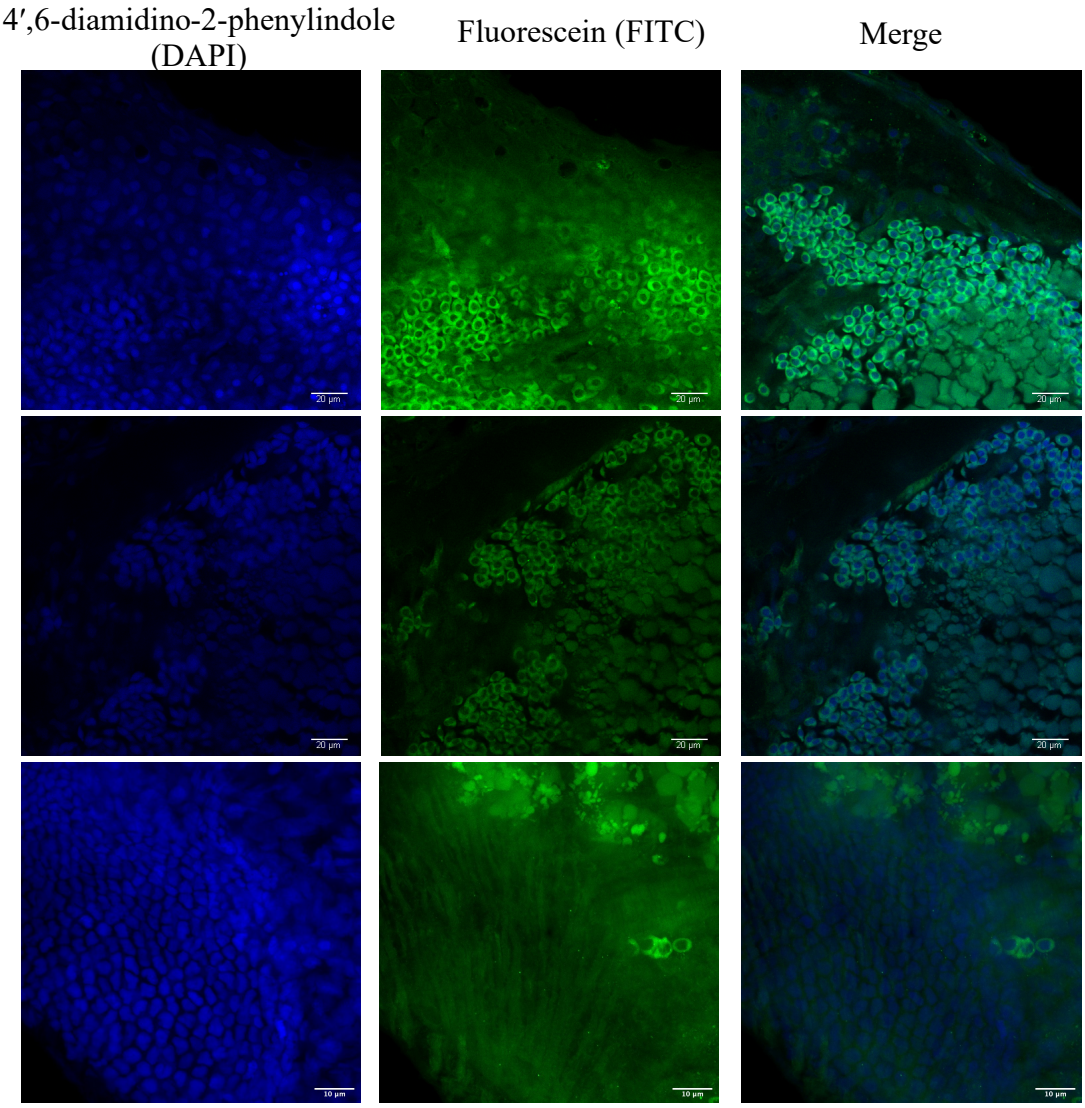

Figure A3. Confocal microscope results of three different samples randomly selected from transfection experiments performed using Lipofectamine-mRNA polyplexes.

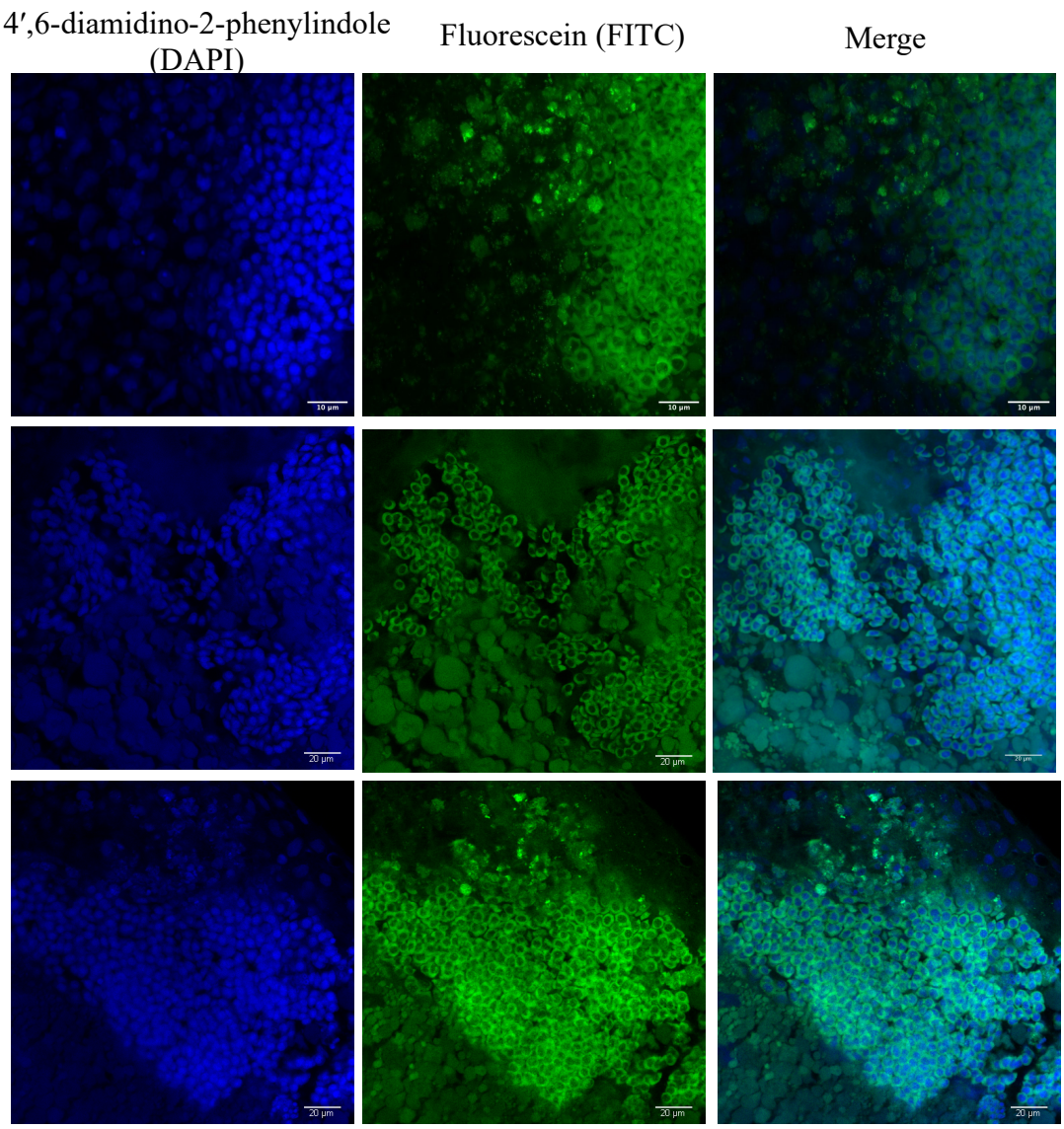

Figure A4. Confocal microscope results of three different samples randomly selected from transfection experiments performed using PEI-mRNA polyplexes with an N/P ratio 50.

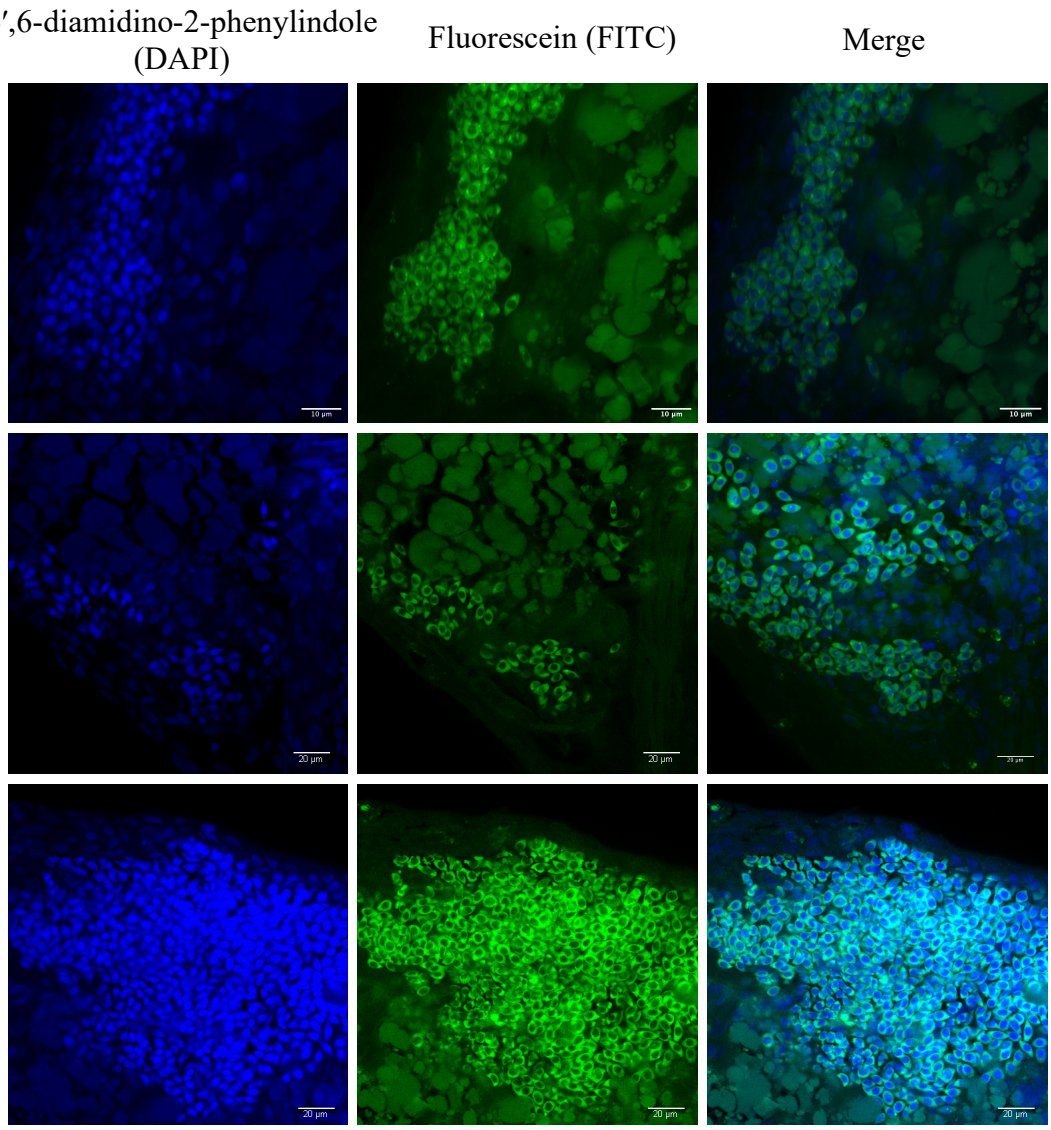

Figure A5. Confocal microscope results of three different samples randomly selected from transfection experiments performed using P(OEGMA)$_{42}$-b-P(AEAEMA)$_{48}$ -mRNA polyplexes with an N/P ratio 3.6.

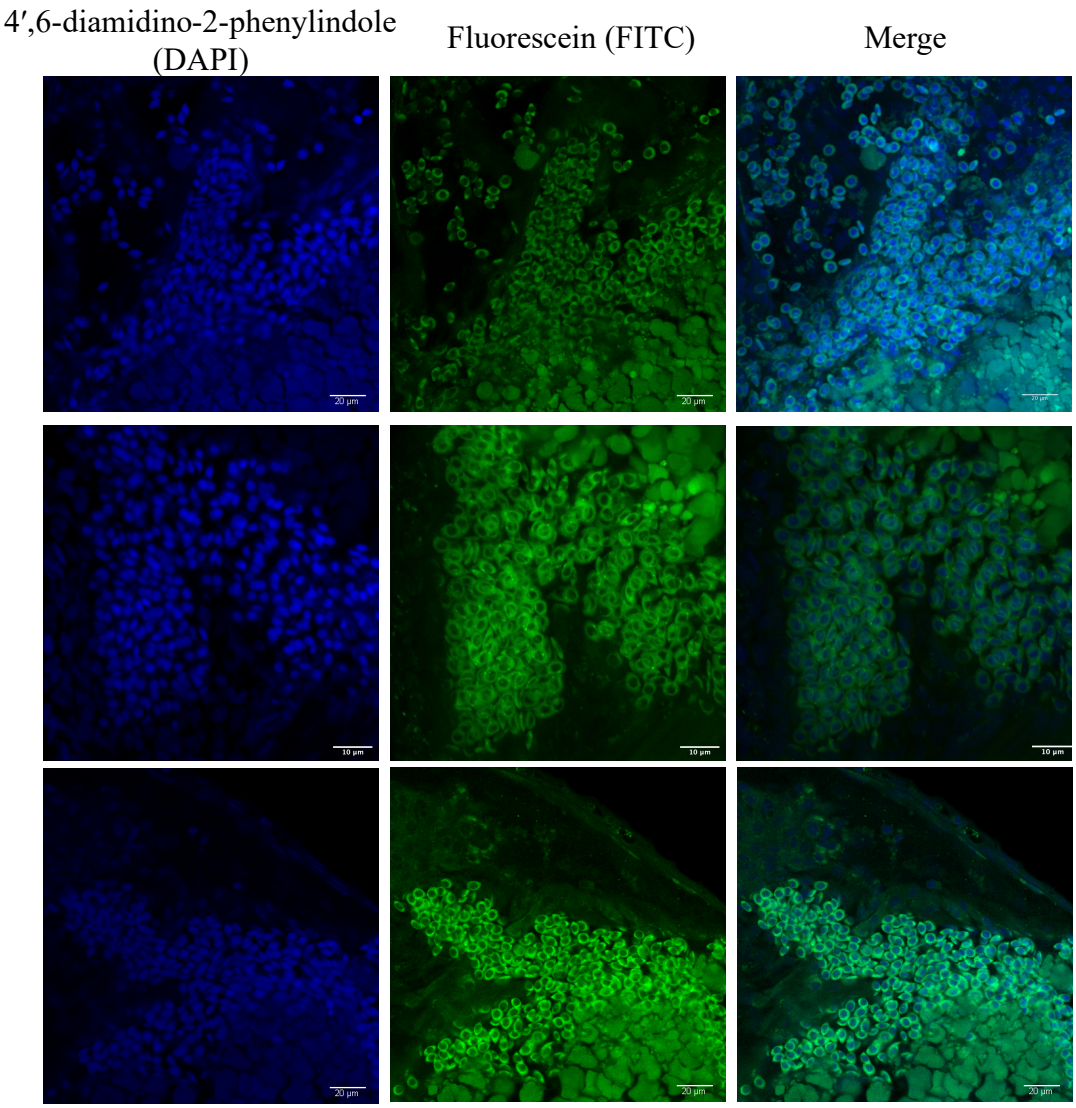

Figure A6. Confocal microscope results of three different samples randomly selected from transfection experiments performed using P(OEGMA)$_{42}$-b-P(AEAEMA)$_{48}$-mRNA polyplexes with an N/P ratio 7.3.

APPENDIX B

IMAGEJ RESULTS OF TRANSFECTION EXPERIMENTS

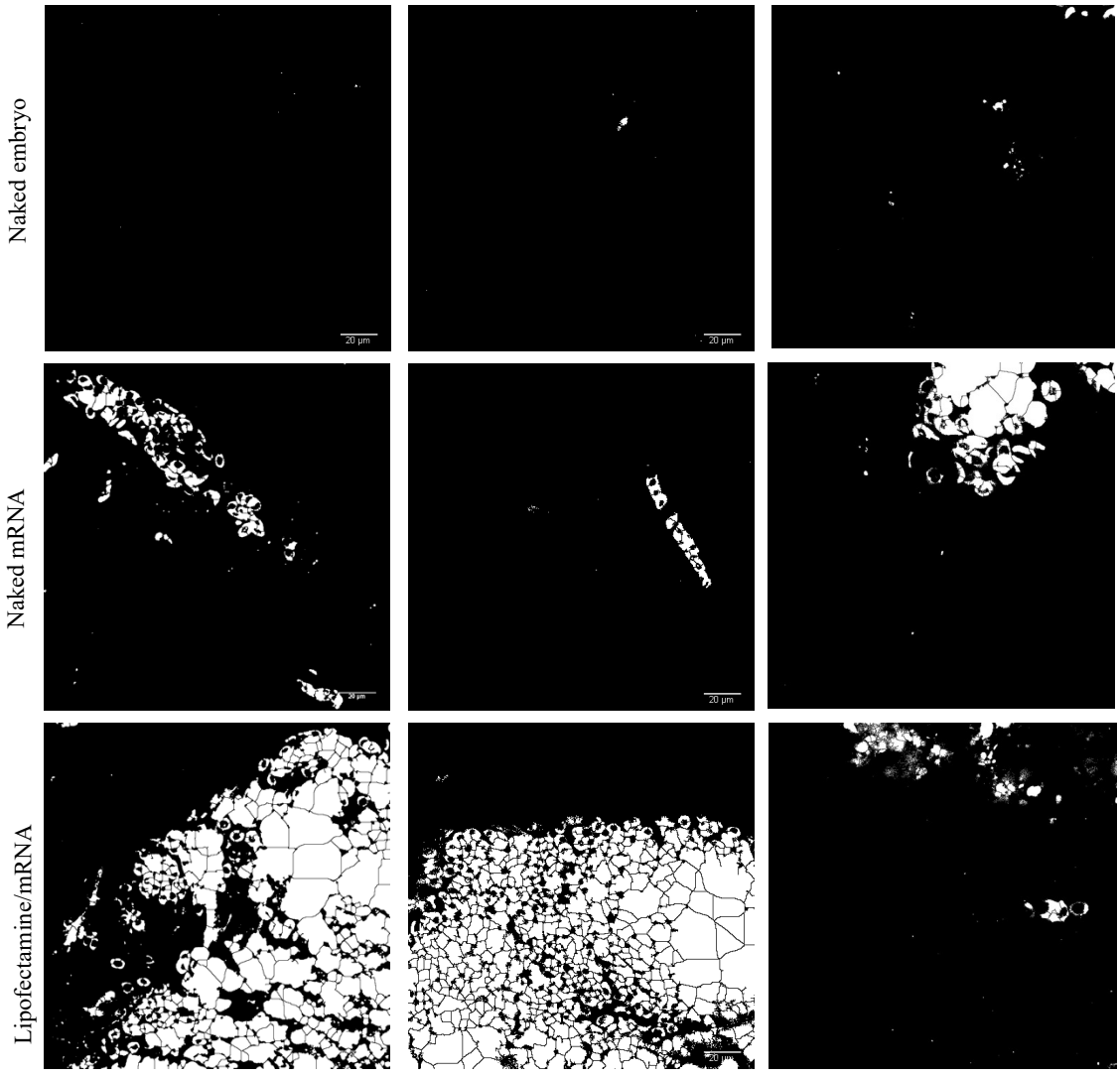

Figure B1. Visualization of three randomly selected overlapping cells analyzed using the threshold function in ImageJ for naked embryo, naked mRNA, and Lipofectamine-mRNA complex.

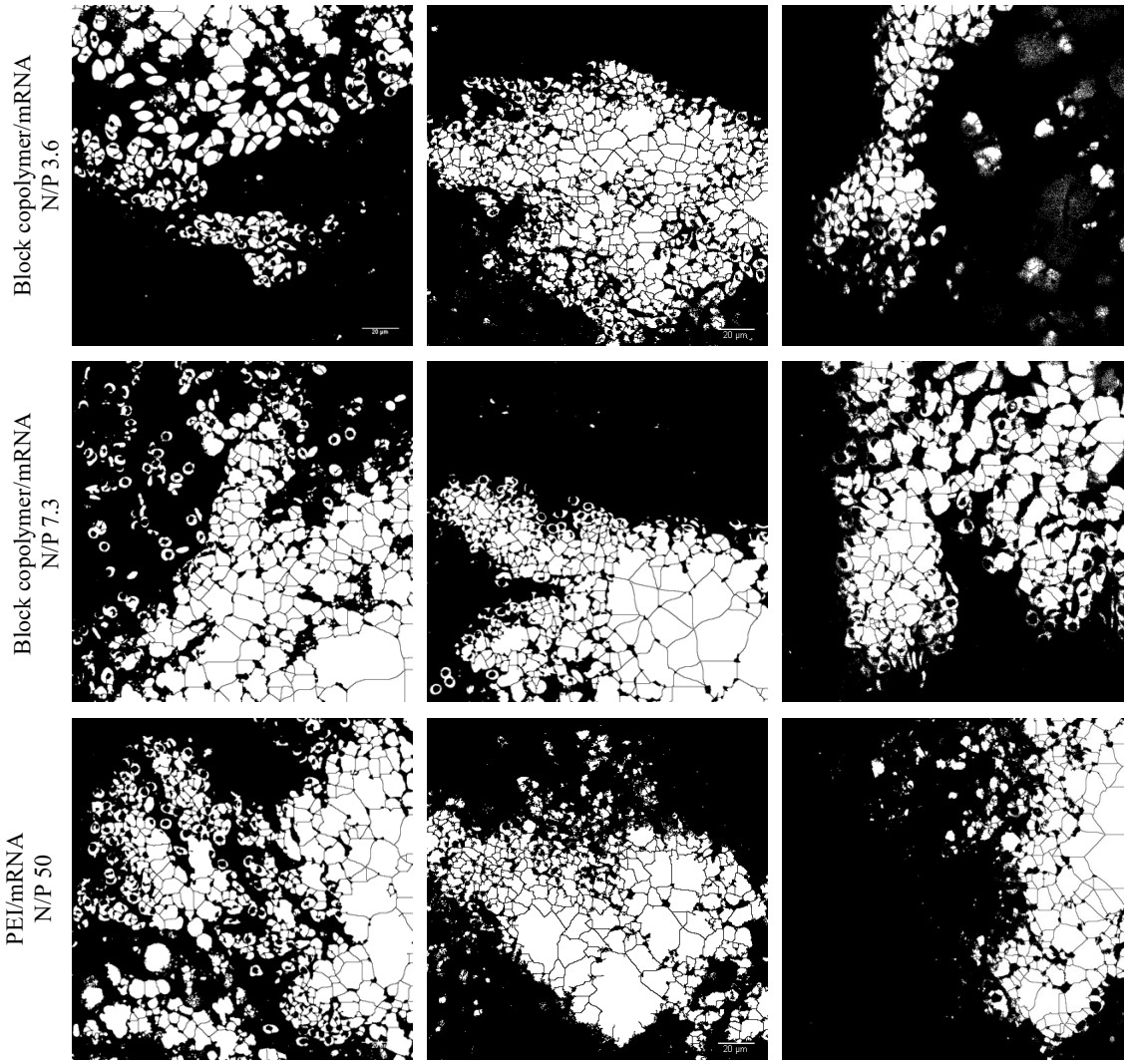

Figure B2. Visualization of three randomly selected overlapping cells analyzed using the threshold function in ImageJ for block copolymer-mRNA (N/P=3.6 and N/P=7.3) and PEI-mRNA (N/P=50).